DETECTION OF DIFFERENT DYNAMICS OF TWO COUPLED OSCILLATORS INCLUDING A TIME-DEPENDENT CUBIC NONLINEARITY

A. Labetoulle
Univ Lyon, ENTPE, LTDS UMR CNRS 5513
3 rue Maurice Audin,
F-69518 Vaulx-en-Velin Cedex, France
`aurelie.labetoulle@entpe.fr`

A. Ture Savadkoohi
Univ Lyon, ENTPE, LTDS UMR CNRS 5513
3 rue Maurice Audin,
F-69518 Vaulx-en-Velin Cedex, France
`alireza.turesavadkoohi@entpe.fr`

E. Gourdon
Univ Lyon, ENTPE, LTDS UMR CNRS 5513
3 rue Maurice Audin,
F-69518 Vaulx-en-Velin Cedex, France
`emmanuel.gourdon@entpe.fr`

January 3, 2022

ABSTRACT

Vibratory energy channelling between a linear and a nonlinear oscillator is studied at different time scales. The nonlinear system possesses a time-dependent periodic restoring forcing function. Detection of fast and slow system dynamics leads to revealing different dynamical characteristics namely slow invariant manifold, equilibrium and singular points. We show that the time-dependent nonlinearity produces phase-dependent slow invariant manifold, frequency responses and modifications concerning stability borders of its slow invariant manifold and singularities zones. The backbone curves of the system and also isola are detected; the later should be taken into account carefully if the aim is system control.

Keywords vibration control · vibratory energy channellig · time-dependent nonlinear rigidity · multiple scales method · equilibrium/singular points

1 Introduction

Most structural systems such as buildings, bridges and vehicles are subjected to vibrations resulting, for example, from traffic, winds, earthquakes and motors, which have different impacts on these systems. Thus, control of vibrations is an important issue as it can prevent fatigue, partial or global damages and even collapse of structural systems and can guarantee their functionalities. Several types of control strategies exist: active, passive and semi-active/passive controls [1]. The active control systems [2] possess sensors that measure movements as well as actuators that generate forces to control vibrations. This type of control technique requires a large amount of external energy. Unlike the active control, the passive control strategy does not need any external power source for its activation and the control process is carried out via direct interactions between the main system and the absorber. Hybrid control systems combine the properties of active and passive absorbers [3]. Semi-active devices are the same as active systems which require less external energy than conventional systems [4, 5]. Semi-passive ones are similar to passive systems but with exploitation of interesting properties of multi-physics systems, for example electro-mechanical devices (e.g. piezoelectric ceramics). These multi-physics systems can be used as sensors and actuators [6]. Their parameters can be changed with a low amount of energy, which give some adaptabilities to the such control systems [7, 8, 9, 10, 11].

Passive control systems are divided into two categories: linear [12] and nonlinear [13]. Linear passive systems can be tuned to a targeted frequency (the mode to be controlled) of the main system. Thus, these control systems are very efficient for narrow frequency ranges. The fact that linear vibration absorbers can act as a vibration amplifiers of the main system for some frequency ranges, was motivation of Roberson [13] to supplement a cubic part to the linear restoring forcing function of the absorber. He showed that the suppression band of a nonlinear absorber is wider compared to a corresponding linear system. Unlike linear systems, pure nonlinear ones do not have especial natural frequencies and can resonate with any frequency. Thus, the nonlinear systems allow to control the vibrations of main systems over wide frequency bands [14]. For such nonlinear systems, the response of the system can be attracted by periodic or non-periodic regimes [15].

One of the nonlinear control systems which were developed in early twenty one century, is named as Nonlinear Energy Sink (NES) [16, 17]. The control process by NES is carried out via nonlinear interactions and (possible) bifurcation(s) between the main system and the NES leading to different regimes. The nonlinearity of the NES in its early developments was pure cubic (without any linear part) [14]. Meanwhile, other types of the NES are developed during the past years, such as vibro-impact [18, 19, 20], piecewise linear [21, 22, 23] and hysteresis systems [24]. The NES in its different forms has been applied in many domains of mechanics and acoustics. In mechanics, it has been applied in controlling linear main system with constant or variable parameters (e.g. time-dependent mass) [25] or nonlinear system (Bouc-Wen model) [26]. In the domain of acoustics, the nonlinear vibro-acoustical energy exchanges between an acoustical mode and a viscoelastic membrane (as a mechanical NES) have been developed by Cochelin et al. [27] and Bellet et al. [28]. Some authors [29, 30, 31] proposed to use a pure acoustical nonlinear absorber to control an acoustical mode. In all those previous studies, the acoustical level of NES activation was very high. That is why some modifications of the system are necessary. Among all possible modifications, an interesting possible option for practical application may be using varying nonlinear stiffness.

That is why in this paper, we are interested in using a NES with a variable cubic rigidity. The considered system can correspond to an acoustical mode which is linearly coupled to an Helmholtz resonator in nonlinear domains [29, 30, 31]. The objective of the paper is to study theoretically this kind of system to be able to provide design tools for tuning parameters and obtaining interesting dynamical regimes for applications.

The paper is organized as it follows: the general methodology for detection of different dynamics of such systems with general nonlinearity is presented in Sect. 2. The explained methodology is applied to the systems with constant and time-dependent cubic nonlinearities in Sects. 3 and 4, respectively. Finally, the paper is concluded in Sect. 5.

2 The general presentation of the system with a general nonlinearity

2.1 General description of the system

The system under consideration is illustrated in Fig. 1. It is composed of two coupled oscillators. The main one is linear which possesses a mass M, a stiffness k_1 and a damper c_1. Its generalized displacement is represented by u_1 and it is submitted to an external force $F(t)$. This oscillator is coupled (by a linear spring γ) to a second nonlinear oscillator with a mass m, a general restoring forcing function Λ and a damper c_2. Its generalized displacement represented by u_2. Moreover, we assume that the mass ratio between two oscillators is small, i.e. $0 < \varepsilon = \dfrac{m}{M} \ll 1$. This system corresponds to an acoustical mode linearly coupled to an absorber with nonlinear behaviour. We consider this system because, until now, most applications of NES in acoustics are mainly realized by a linear coupling term between the main system and the nonlinear oscillator [28, 32, 30], while in mechanics the coupling is generally nonlinear [14]. The governing equations of the system at the time t are:
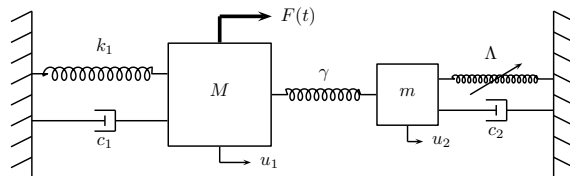

Figure 1: The system under consideration: the linear oscillator with the mass M is linearly coupled to a nonlinear oscillator with the mass m and a general nonlinear restoring forcing function Λ.

$$\begin{cases} M\ddot{u}_1 + k_1 u_1 + c_1 \dot{u}_1 + \gamma(u_1 - u_2) = F(t) \\ m\ddot{u}_2 + c_2 \dot{u}_2 + \gamma(u_2 - u_1) + \Lambda(u_2) = 0 \end{cases} \tag{1}$$

We set that $(\dot{\cdot}) = \dfrac{\partial}{\partial t}$. Let us introduce the new time τ as:

$$\tau = t\sqrt{\frac{k_1}{M}} = t\omega_1 \tag{2}$$

and we set that $(\cdot)' = \dfrac{\partial}{\partial \tau}$. Following equations is obtained in the time domain τ:

$$\begin{cases} u_1'' + u_1 + \varepsilon\xi_1 u_1' + \varepsilon\gamma_0(u_1 - u_2) = \varepsilon f_0 \sin(\nu\tau) \\ \varepsilon u_2'' + \varepsilon\xi_2 u_2' + \varepsilon\gamma_0(u_2 - u_1) + \varepsilon\Lambda_0(u_2) = 0 \end{cases} \tag{3}$$

Where $\dfrac{c_1}{\sqrt{k_1 M}} = \varepsilon\xi_1;\ \dfrac{\gamma}{k_1} = \varepsilon\gamma_0\ ;\ \dfrac{\Lambda(u_2)}{k_1} = \varepsilon\Lambda_0(u_2)\ ;\ \dfrac{F_0}{k_1} = \varepsilon f_0\ ;\ \dfrac{c_2}{\sqrt{k_1 M}} = \varepsilon\xi_2\ ;\ \dfrac{\Omega}{\omega_1} = \nu$. The orders of magnitude are chosen to according to practical applications.

We are interested in studying system behaviours in the vicinity of the 1:1 resonance; consequently we set $\nu = 1 + \sigma\varepsilon$.

In the next subsections, the system variables will be complexified and via a time multiple scales method [33], different system dynamics [34] will be detected.

2.2 Complexifications

Let us introduce the complex variables of Manevitch [35, 36] ($i^2 = -1$):

$$\begin{cases} \phi_1 e^{i\nu\tau} = u_1' + i\nu u_1 \\ \phi_2 e^{i\nu\tau} = u_2' + i\nu u_2 \end{cases} \tag{4}$$

The multiple scales method [33] is used to detect different dynamics of the system. We introduce different scales of time: $T_0 = \tau$ (fast time scale) and $T_j = \varepsilon^j \tau$ ($j = 1, 2...$) (slow time scales). These time scales are coupled to each other via the mass ratio of two oscillators, i.e. the ε parameter. With these definitions of different time scales, we have:

$$\frac{\partial}{\partial \tau} = \frac{\partial}{\partial T_0} + \varepsilon\frac{\partial}{\partial T_1} + ... \tag{5}$$

We use the Galerkin method to keep only first harmonics of the system and to truncate other ones. For an arbitrary function $s(\phi_1, \phi_2, \phi_1^*, \phi_2^*)$ this task is carried out via:

$$S(\phi_1, \phi_2, \phi_1^*, \phi_2^*) = \frac{\nu}{2\pi} \int_0^{\frac{2\pi}{\nu}} s(\phi_1, \phi_2, \phi_1^*, \phi_2^*) e^{-ji\omega\tau} d\tau \tag{6}$$

with $j = 1$. The (.)* represents the complex conjugate of a variable.

In applying Eq. (6), we will suppose that $\phi_1, \phi_2, \phi_1^*, \phi_2^*$ are independent of the fast time $T_0 = \tau$. This hypothesis will be verified during the multiple scales method or when we will consider an asymptotic state when $T_0 \to +\infty$ (Sect. 2.3.1).

After using the Galerkin method via applying Eqs. (6), Eq. (3) reads:

$$\begin{cases} \phi_1' + \dfrac{i}{2}\nu\phi_1 + \dfrac{1}{2}\varepsilon\xi_1\phi_1 + \dfrac{1}{2i\nu}\phi_1 + \varepsilon\gamma_0\dfrac{1}{2i\nu}(\phi_1 - \phi_2) = \dfrac{\varepsilon f_0}{2i} \\ \varepsilon\left(\phi_2' + \dfrac{i}{2}\nu\phi_2\right) + \dfrac{1}{2}\varepsilon\xi_2\phi_2 + \varepsilon\gamma_0\dfrac{1}{2i\nu}(\phi_2 - \phi_1) + \varepsilon G(u_2) = 0 \end{cases} \tag{7}$$

with

$$G(u_2) = \frac{\nu}{2\pi} \int_0^{\frac{2\pi}{\nu}} \Lambda_0(u_2) e^{-i\nu\tau} d\tau \tag{8}$$

As ε is a small parameter ($0 < \varepsilon \ll 1$), the different terms of Eq. (7) can be developed in terms of Taylor series in ε.

2.3 Detection of fast and slow dynamics of the system

To detect fast and slow dynamics of the system, Eq. (7) will be treated by the multiple scales method [33] via studying system equations at different orders of ε. The global idea is to provide design tools for tuning parameters of the nonlinear oscillator. These tools are based on the vision of the evaluation of the slow invariant manifold (SIM) of the system [37] and detection of all of its characteristic points (equilibrium and singular points) around the SIM [38]. They will lead to prediction of periodic and non-periodic regimes of the system for given intervals of deriving forcing amplitudes and frequencies.

However, there are many works which use multiple scales method for finding solutions of system variables or detection of periodic regimes (e.g. see [39, 40, 41, 42, 43, 44, 45, 46]), which is not the aim of this paper.

2.3.1 Fast system dynamics: $O(\varepsilon^0)$ of system equations

Here, we consider the behaviour of the system at fast time scale. Equation (7) at $O(\varepsilon^0)$ reads:

$$
\begin{cases}
\dfrac{\partial \phi_1}{\partial T_0} = 0 & (9.1) \\[2mm]
\dfrac{\partial \phi_2}{\partial T_0} + \mathscr{H}(\phi_1, \phi_1^*, \phi_2, \phi_2^*) = 0 & (9.2)
\end{cases}
\tag{9}
$$

The hypothesis $\dfrac{\partial \phi_1}{\partial T_0} = 0$ is verified. Let us seek for fixed points of the system. This means that we would like to detect an asymptotic state when $T_0 \to +\infty$, i.e. $\dfrac{\partial \phi_2}{\partial T_0} = 0$. It leads to:

$$
\mathscr{H}(\phi_1, \phi_2, \phi_1^*, \phi_2^*) = \frac{1}{2}i\phi_2 + \frac{1}{2}\xi_2\phi_2 - \frac{i\gamma_0}{2}(\phi_2 - \phi_1) + G(u_2) = 0
\tag{10}
$$

Equation (10) is called Slow Invariant Manifold (SIM) in the complex domain. Let us consider the complex variables in the polar domain as:

$$
\phi_j = N_j e^{i\delta_j}
\tag{11}
$$

$N_j \in \mathbb{R}_+$ and $\delta_j \in \mathbb{R}$, $j = 1, 2$ with N_j the amplitude and δ_j the phase of ϕ_j. Let us assume that after applying Eq. (11) in Eq. (10), the SIM in real domain reads:

$$
H(N_1, \delta_1, N_2, \delta_2) = 0
\tag{12}
$$

2.3.2 Detection of unstable zone of the SIM

In this section, the unstable zone of the SIM will be determined. To carry out the stability analysis of the SIM, we linearly perturb system variables as:

$$
\begin{cases}
\phi_2 \to \phi_2 + \Delta\phi_2 \\
\phi_2^* \to \phi_2^* + \Delta\phi_2^*
\end{cases}
\tag{13}
$$

with $|\Delta\phi_2| \ll |\phi_2|$. We do not perturb ϕ_1 as $\dfrac{\partial \phi_1}{\partial T_0} = 0$ (see Eq. (9)).

The perturbation is introduced in Eq. (9.2). This leads to the following system:

$$
\begin{pmatrix}
\dfrac{\partial \Delta\phi_2}{\Delta T_0} \\[4mm]
\dfrac{\partial \Delta\phi_2^*}{\Delta T_0}
\end{pmatrix}
= \mathbb{M}
\begin{pmatrix}
\Delta\phi_2 \\
\Delta\phi_2^*
\end{pmatrix}
\tag{14}
$$

The eigenvalues of the matrix $\mathbb{M}$ can be calculated to determine the boundaries of the unstable zone of the SIM.

2.3.3 Slow system dynamics: $O(\varepsilon)$ of system equations

In this subsection, we consider the system behaviour at the slow time scale and we will detect the equilibrium and singular points. The first equation of the system (7) at $O(\varepsilon)$ reads:

$$\frac{\partial \phi_1}{\partial T_1} = \underbrace{-\frac{if_0}{2} - \left[\frac{1}{2} i\sigma\phi_1 + \frac{1}{2}\xi_1\phi_1 + \frac{1}{2}i\sigma\phi_1 - \frac{i\gamma_0}{2}(\phi_1 - \phi_2) \right]}_{\mathcal{E}(\phi_1,\phi_2,\phi_1^*,\phi_2^*)} \tag{15}$$

Then, the evolution of the SIM (see Eq. (10)) at the time scale T_1 is developed as:

$$\begin{cases} \dfrac{\partial \mathscr{H}}{\partial T_1} = \dfrac{\partial \mathscr{H}}{\partial \phi_1}\dfrac{\partial \phi_1}{\partial T_1} + \dfrac{\partial \mathscr{H}}{\partial \phi_2}\dfrac{\partial \phi_2}{\partial T_1} + \dfrac{\partial \mathscr{H}}{\partial \phi_1^*}\dfrac{\partial \phi_1^*}{\partial T_1} + \dfrac{\partial \mathscr{H}}{\partial \phi_2^*}\dfrac{\partial \phi_2^*}{\partial T_1} = 0 \\[2mm] \dfrac{\partial \mathscr{H}^*}{\partial T_1} = \dfrac{\partial \mathscr{H}}{\partial \phi_1}\dfrac{\partial \phi_1}{\partial T_1} + \dfrac{\partial \mathscr{H}^*}{\partial \phi_2}\dfrac{\partial \phi_2}{\partial T_1} + \dfrac{\partial \mathscr{H}^*}{\partial \phi_1^*}\dfrac{\partial \phi_1^*}{\partial T_1} + \dfrac{\partial \mathscr{H}^*}{\partial \phi_2^*}\dfrac{\partial \phi_2^*}{\partial T_1} = 0 \end{cases} \tag{16}$$

After some mathematical manipulations, Eq. (16) in matrix form reads:

$$\underbrace{\begin{bmatrix} \dfrac{\partial \mathscr{H}}{\partial \phi_2} & \dfrac{\partial \mathscr{H}}{\partial \phi_2^*} \\[2mm] \dfrac{\partial \mathscr{H}^*}{\partial \phi_2} & \dfrac{\partial \mathscr{H}^*}{\partial \phi_2^*} \end{bmatrix}}_{\mathbb{A}} \begin{bmatrix} \dfrac{\partial \phi_2}{\partial T_1} \\[2mm] \dfrac{\partial \phi_2^*}{\partial T_1} \end{bmatrix} = - \begin{bmatrix} \dfrac{\partial \mathscr{H}}{\partial \phi_1} & \dfrac{\partial \mathscr{H}}{\partial \phi_1^*} \\[2mm] \dfrac{\partial \mathscr{H}^*}{\partial \phi_1} & \dfrac{\partial \mathscr{H}^*}{\partial \phi_1^*} \end{bmatrix} \begin{bmatrix} \dfrac{\partial \phi_1}{\partial T_1} \\[2mm] \dfrac{\partial \phi_1^*}{\partial T_1} \end{bmatrix} \tag{17}$$

Equilibrium points are defined by [38] :

$$\begin{cases} \mathcal{E}(\phi_1, \phi_2, \phi_1^*, \phi_2^*) = 0 \\ \mathscr{H}(\phi_1, \phi_2, \phi_1^*, \phi_2^*) = 0 \\ \det(\mathbb{A}) \neq 0 \end{cases} \tag{18}$$

Singular points are defined by [38] :

$$\begin{cases} \mathcal{E}(\phi_1, \phi_2, \phi_1^*, \phi_2^*) = 0 \\ \mathscr{H}(\phi_1, \phi_2, \phi_1^*, \phi_2^*) = 0 \\ \det(\mathbb{A}) = 0 \end{cases} \tag{19}$$

After providing a general methodology for detection of different dynamics of explained coupled oscillators, the application of the method will be shown for a nonlinear system with constant and time-dependent cubic nonlinearities.

3 Detection of different dynamics of the system with constant cubic nonlinearity

Here, we apply the general methodology described in the Sect. 2 to study the energy exchanges between two oscillators where one of them possesses a constant cubic nonlinearity. Such systems have been already studied and also applied in many domains such as civil engineering [47, 48, 49], aeroelastic/aerospace systems [50, 51, 52, 53, 54] and acoustic [27, 28]. In the following we give details to be able to compare the results with the case of variable rigidity which will be treated in the Sect. 4.

3.1 General presentation of the system

Let us assume that the stiffness of the nonlinear oscillator is constant and it presents cubic behaviour, i.e. $\Lambda(u_2) = k_2 u_2^3$, as presented in Fig. 1.

We suppose that $\dfrac{k_2}{k_1} = \varepsilon k_0$. The $G(u_2)$ function of Eq. (7) becomes:

$$G(\phi_2, \phi_2^*) = \frac{-3ik_0}{8\nu^3}\phi_2|\phi_2|^2 \tag{20}$$

In the following subsection, we will consider Eq. (7) at different orders of ε to detect the fast and slow dynamic of the system [34].

3.2 Fast system dynamics

To detect the fast dynamic of the system, $O(\varepsilon^0)$ of Eq. (7) should be investigated. This leads to similar equations as shown in Eq. (9). Here, we have:

$$\mathscr{H} = \frac{1}{2}i\phi_2 + \frac{1}{2}\xi_2\phi_2 - \frac{i\gamma_0}{2}(\phi_2 - \phi_1) - \frac{3}{8}ik_0\phi_2|\phi_2|^2 = 0 \tag{21}$$

Hence,

$$\phi_1 = \frac{\phi_2}{\gamma_0}\left(-1 + i\xi_2 + \gamma_0 + \frac{3}{4}k_0|\phi_2|^2\right) \tag{22}$$

Going to the polar domain as explained in Eq. (11) and after separation of real and complex parts, the equations of the SIM in the real domain reads:

$$N_1 = \frac{N_2}{\gamma_0}\sqrt{\xi_2^2 + \left(-1 + \gamma_0 + \frac{3}{4}k_0N_2^2\right)^2} \tag{23}$$

$$\delta_1 = \delta_2 + \arctan\left(\frac{\xi_2}{-1 + \gamma_0 + \frac{3}{4}k_0N_2^2}\right) \tag{24}$$

To determine the local extrema of the SIM, we seek $\frac{\partial N_1^2}{\partial N_2^2} = 0$. After some mathematical manipulations, we obtain:

$$\frac{27}{6}k_0^2X^2 - 3(1 - \gamma_0)k_0X + (1 - \gamma_0)^2 + \xi_2^2 = 0 \tag{25}$$

with $X = N_2^2$. The solutions of Eq. (25) are:

$$X_{1,2} = \frac{(1 - \gamma_0) \mp \frac{1}{2}\sqrt{(1 - \gamma_0)^2 - 3\xi_2^2}}{\frac{9}{8}k_0} \tag{26}$$

Hence, if $(1 - \gamma_0)^2 - 3\xi_2^2 \geq 0$ the local extrema of the SIM correspond to $N_{2,1} = \sqrt{X_1}$ and $N_{2,2} = \sqrt{X_2}$. Otherwise, if $(1 - \gamma_0)^2 - 3\xi_2^2 < 0$, the SIM does not possess local extrema.

3.3 Unstable zones of the SIM

To determine the boundaries of the unstable zones, we investigate Eq. (9.2); it reads:

$$\frac{\partial\phi_2}{\partial T_0} + \frac{1}{2}\phi_2\left(i\left(1 - \gamma_0 - \frac{3}{4}k_0|\phi_2|^2\right) + \xi_2\right) + i\frac{\gamma_0}{2}\phi_1 = 0 \tag{27}$$

After taking into account the complex conjugate of Eq. (27), and introducing the perturbed from of variables (see Eq. (13)), we obtain the following equation:

$$\begin{pmatrix} \dfrac{\partial\Delta\phi_2}{\Delta T_0} \\[3mm] \dfrac{\partial\Delta\phi_2^*}{\Delta T_0} \end{pmatrix} = \frac{1}{2}\underbrace{\begin{pmatrix} -i\left(1 - \gamma_0 - \frac{3}{4}k_0|\phi_2|^2\right) - \xi_2 & \frac{3}{4}ik_0\phi_2^2 \\[3mm] -\frac{3}{4}ik_0\phi_2^{*2} & i\left(1 - \gamma_0 - \frac{3}{4}k_0|\phi_2|^2\right) - \xi_2 \end{pmatrix}}_{\mathbb{M}}\begin{pmatrix} \partial\Delta\phi_2 \\[3mm] \partial\Delta\phi_2^* \end{pmatrix} \tag{28}$$

The eigenvalues (λ) of the matrix $\mathbb{M}$ are evaluated to analyse the stability of the SIM:

$$\left(\mathbb{M}_{11} - \lambda\right)\left(\mathbb{M}_{22} - \lambda\right) - \frac{9}{64}k_0^2|\phi_2|^4 = 0 \tag{29}$$

which lead to:

$$\lambda^2 - \alpha\lambda + \beta = 0 \tag{30}$$

with $\alpha = \left(\mathbb{M}_{11} + \mathbb{M}_{22}\right)$ and $\beta = \mathbb{M}_{11}\mathbb{M}_{22} - \frac{9}{64}k_0^2|\phi_2|^4$.

If λ_1 and λ_2 are solutions of Eq. (30), then we can claim:

$$\begin{cases} \lambda_1 + \lambda_2 & = \alpha = -\xi_2 < 0 \\ \lambda_1\lambda_2 & = \beta \end{cases} \tag{31}$$

The system is stable if the real parts of λ_1 and λ_2 are negatives. We distinguish two global cases:

- if $\beta > 0$ then, the eigenvalues can be complex or real:
    - if they are real, they should be negative, so fixed points are stable.
    - if they are complex, then they share the same real negative parts equal to $\frac{\alpha}{2}$. So, fixed points are stable.
- if $\beta < 0$ then, real part of λ_1 or λ_2 is positive, so the system is unstable.

As a summary, the condition $\beta = 0$, clarifies boundaries between stable and unstable zones of the SIM. Let us set $X = N_2^2$. The condition of $\beta = 0$ leads to the same equation as the one of the extrema of the SIM (see Eq. (25)). Hence, $N_{2,1} = \sqrt{X_1}$ and $N_{2,2} = \sqrt{X_2}$ (see Eq. (26)) correspond to the boundaries of the unstable zone. Consequently, we see that the stability borders of the SIM pass from its local extrema (see Eq. (26)).

3.4 Slow system dynamics

3.4.1 Singular points

Let us build the matrix $\mathbb{A}$ from the Eq. (21) which is explained in Eq. (17):

$$\mathbb{A} = \frac{1}{2}\begin{bmatrix} \xi_2 - i\left(-1 + \gamma_0 + \frac{3}{2}k_0|\phi_2|^2\right) & -\frac{3}{4}ik_0\phi_2^2 \\ \frac{3}{4}ik_0\phi_2^{*2} & \xi_2 + i\left(-1 + \gamma_0 + \frac{3}{2}k_0|\phi_2|^2\right) \end{bmatrix} \tag{32}$$

So,

$$\det\left(\mathbb{A}\right) = 0 \Rightarrow \xi_2^2 + \left(1 - \gamma_0 - \frac{3}{2}k_0N_2^2\right)^2 - \left(\frac{3}{4}k_0N_2^2\right)^2 = 0 \tag{33}$$

Let us set $X = N_2^2$. Equation (33) yields to:

$$\frac{27}{16}k_0^2X^2 + (1 - \gamma_0)^2 + 3(-1 + \gamma_0)k_0X + \xi_2^2 + (1 - \gamma_0)^2 = 0 \tag{34}$$

Thus, the two real solutions of Eq. (34) are the same which are presented in Eq. (26). So, positions of possible singular points of the system will be on $N_{2,1} = \sqrt{X_1}$ and $N_{2,2} = \sqrt{X_2}$. Then, in addition to Eq. (33), other two conditions of Eq. (19) should be verified as well in order to have confirmation of existence of singularities in system for given σ and f_0 [55].

In order to have two distinct solutions described in Eq. (26), the rescaled damping of the nonlinear oscillator must not exceed a critical value namely $\xi_{2,c}$, which is defined as:

$$\xi_{2,c} = \frac{1}{\sqrt{3}}(1 - \gamma_0) \tag{35}$$

If $\xi_2 > \xi_{2,c}$, the SIM becomes monotonic and it does not possess singular points nor local extrema. A similar condition for mechanical systems has been already detected by Starosvetsky and Gendelman [56]. Figure 2 shows the SIM for different values of ξ_2. The red dotted, black solid, blue dashed and green circled lines represent the SIM for $\xi_2 = 0$, $\xi_2 < \xi_{2,c}$, $\xi_2 = \xi_{2,c}$ and $\xi_2 > \xi_{2,c}$, respectively.
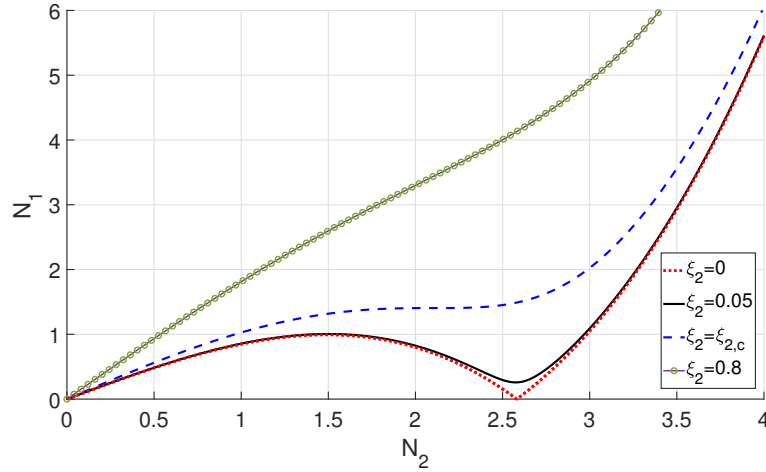

Figure 2: The SIM for different values of ξ_2: $\xi_2 = 0$ (red dotted line), $\xi_2 = 0.05 < \xi_{2,c}$ (black solid line), $\xi_2 = \xi_{2,c}$ (blue dashed line) and $\xi_2 = 0.8 > \xi_{2,c}$ (green circled line). System parameters are reported in Table 1.

The associated values of N_1 with $N_{2,1}$ and $N_{2,2}$ can be calculated using the SIM equation (see Eq. (23)). Thus, the geometrical places of possible singularities can be clarified completely. Figure 3 shows the SIM of the system with its unstable zone (green) and the geometrical places of singular points. We consider the parameters defined in the Table 1. We observe that the singular points are located on the boundaries of the unstable zone and also on the position of local extrema of the SIM.

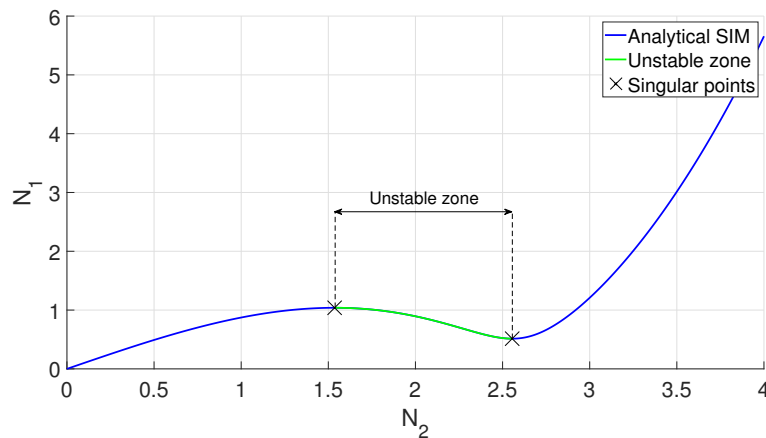| Parameter	Value
k_0	0.1
ξ_2	0.1
γ_0	0.5

Table 1: Parameters of the system.

Figure 3: The SIM of the system accompanied by its unstable zone (green) and positions of singularities ($\times$).

3.4.2   Detection of equilibrium points of the system

To find equilibrium points of the system, we seek for those values of N_2 when $\mathcal{E}$ in Eq. (15) becomes zero.

Via injection of Eq. (22) in Eq. (15) and after some mathematical manipulations we have (see Appendix A):

$$aX^3 + bX^2 + cX + d = 0 \tag{36}$$

with $X = N_2^2$ and

$$
\begin{cases}
a = & \left(\dfrac{3}{4}k_0\right)^2 \left[\xi_1^2 + (2\sigma - \gamma_0)^2\right] \\
b = & \dfrac{3}{2}k_0 \left[(-1 + \gamma_0)\left[\xi_1^2 + (2\sigma - \gamma_0)^2\right] + (2\sigma - \gamma_0)\gamma_0^2\right] \\
c = & (-1 + \gamma_0)^2 \left[\xi_1^2 + (2\sigma - \gamma_0)^2\right] + 2(-1 + \gamma_0)(2\sigma - \gamma_0)\gamma_0^2 + \left(\xi_1\xi_2 + \gamma_0^2\right)^2 + (2\sigma - \gamma_0)^2\xi_2^2 \\
d = & -f_0^2\gamma_0^2
\end{cases} \tag{37}
$$

Equation (36) can be solved with the Cardano's method. So, we can find the N_2 values for which correspond to equilibrium or singular points. Then, one can obtain N_1 from detected N_2 by Eq. (23).

3.4.3   Detection of the backbone curve of the system

To determine the backbone curve of the system, we seek for periodic responses of the undamped system without any external excitation. That is to say in Eq. (36) we set $f_0 = 0$ and $\xi_1 = \xi_2 = 0$ (see Eq. (3)). It reads:

$$a_{bc}X^2 + b_{bc}X + c_{bc} = 0 \tag{38}$$

with

$$
\begin{cases}
a_{bc} = & \left(\dfrac{3}{4}k_0(2\sigma - \gamma_0)\right)^2 \\
b_{bc} = & \dfrac{3}{2}k_0(2\sigma - \gamma_0)\left[2\sigma(-1 + \gamma_0) + \gamma_0\right] \\
c_{bc} = & (-1 + \gamma_0)(2\sigma - \gamma_0)\left[(-1 + \gamma_0)(2\sigma - \gamma_0) + 2\gamma_0^2\right] + \gamma_0^4
\end{cases} \tag{39}
$$

As $X = N_2^2$, then we should admit only real and positive solutions of X in Eq. (38). For a sweeping detuning parameter σ, Eq. (38) can be solved easily to collect real and positive solutions as $N_2 = \sqrt{X}$. The associate values of N_1 can be obtained from the equation of the SIM (see Eq. (23)).

3.5   Numerical results

Let us consider system parameters which are presented in Table 2. The equilibrium points obtained from Eq. (36) for sweeping σ are illustrated on Fig. 4a. These curves are in fact the frequency response of the system. Different two-dimension views of Fig. 4a are depicted in Figs. 4b-4d. Figure 4b projects the possible parts of the SIM which cover the equilibrium points for the system under external excitation amplitude $f_0 = 1.1$. Figures 4c and 4d show the amplitudes of equilibrium points (N_1 and N_2) as functions of the σ parameter. The green parts in these figures correspond to the unstable zone of the SIM. For this example, we observe that the frequency response curve possesses a main branch and an isola. Depending on the value of σ, one, two or three equilibrium points exist which could be stable or unstable. To check the validity of obtained analytical predictions, we carry out numerical integrations of the governing equations of the system (see Eq. (3)) with the Runge-Kutta method.

Parameter	Value
k_0	0.1
ξ_1	0.1
ξ_2	0.1
γ_0	0.5
ε	0.01

Table 2: Parameters of the system.

3.5.1   Analytical predictions versus resultats of direct numerical integrations

Here, we provide some examples where the system possesses only one equilibrium point, e.g. for $\sigma = 1$, and three equilibrium points, e.g. for $\sigma = -0.3$ (see Fig. 4).
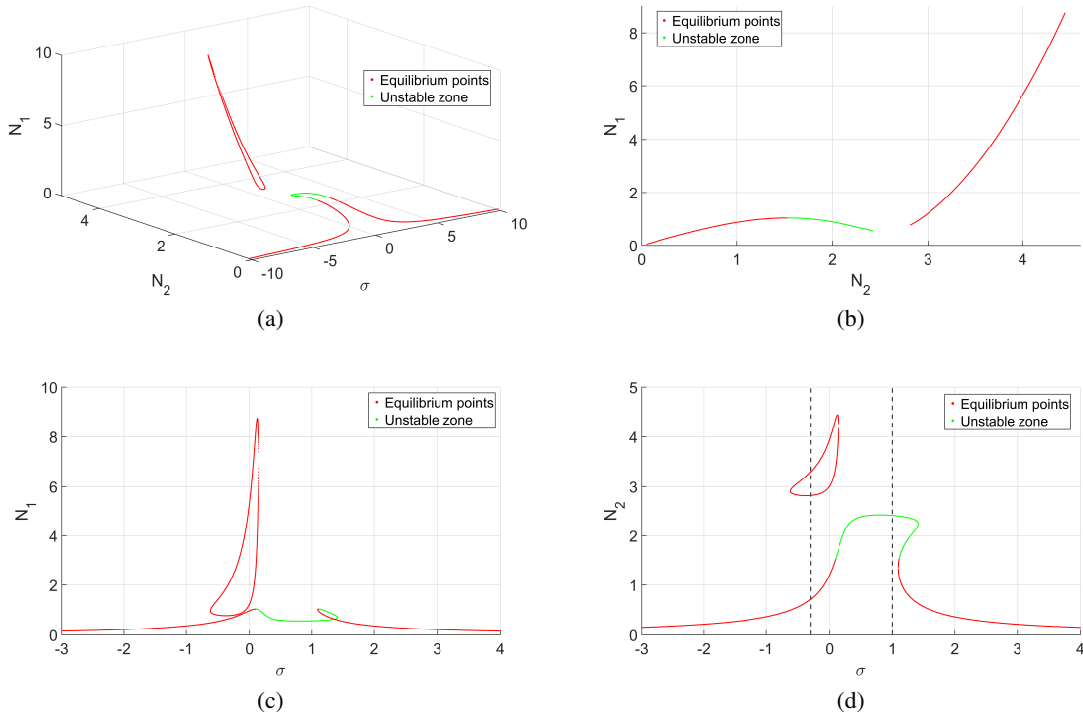
(a)

(b)

(c)

(d)

Figure 4: Equilibrium points of the system (Table 2, $f_0 = 1.1$) for sweeping detuning parameters σ. a) Three-dimensional view (σ, N_2, N_1); b) Two-dimensional view (N_1, N_2); c) Two-dimensional view (σ, N_1) and d) Two-dimensional view (σ, N_2). Located equilibrium points in unstable zone of the SIM are represented by the green line.

- $\sigma = 1$

  For $\sigma = 1$, there is only one equilibrium point as $(N_2, N_1) = (2.41, 0.57)$, which is in the unstable zone of the SIM (see Fig. 4). We suppose following initial conditions: $(u_1(\tau = 0), u_2(\tau = 0), u_1'(\tau = 0), u_2'(\tau = 0)) = (0, 0, 0, 0)$. Figure 5a collects results obtained from direct numerical integration (blue line), the SIM (red line) and the initial conditions (black point). Time histories of system responses are illustrated in Figs. 5b and 5c. Figure 5 indicates that the system presents a Strongly Modulated Response (SMR) [56] which corresponds to repeated bifurcations between the stable branches of the SIM. This is because of positioning of equilibrium point in the unstable area of the SIM.

- $\sigma = -0.3$

  For $\sigma = -0.3$, there are three equilibrium points: one on the main branch namely, (i) $(N_2, N_1) = (0.71, 0.67)$ and two others on the isola namely, (ii) $(N_2, N_1) = (2.82, 0.78)$ and (iii) $(N_2, N_1) = (3.30, 2.19)$ (see Fig. 4). We will carry out two numerical integrations with following initial conditions:

  - $(u_1(\tau = 0), u_2(\tau = 0), u_1'(\tau = 0), u_2'(\tau = 0)) = (0, 0, 0, 0)$ (see Fig. 6). The system is attracted by the equilibrium point (i) located on the main branch (dotted lines in Fig. 6a).
  - $(u_1(\tau = 0), u_2(\tau = 0), u_1'(\tau = 0), u_2'(\tau = 0)) = (2.2, 3.4, 0, 0)$: these initial conditions are close to the equilibrium point (iii) located at the upper part of the isola. Figure 7 shows that the system is attracted by this point (dotted lines in Fig. 7a).

3.5.2 The backbone curve of the system

Figure 2 shows the backbone curve of the system with $k_0 = 0.1$ and $\gamma_0 = 0.5$. This figure is obtained from Eq. (38) and collects two branches namely, (I) and (II). The two-dimensional view of the Fig. 8a is presented in Fig. 8b. This curve is in fact the SIM of the undamped system which is presented in Fig. 2. The frequency response curves of the system (parameters of the Table 2) under different forcing amplitudes, namely $f_0 = 0.7$, $f_0 = 1.1$ and $f_0 = 1.5$ are added to the same figure and are illustrated in Fig. 9. It is seen that the backbone curve collects (almost) local maxima of the frequency response curves. Moreover, if the forced system presents possible isola, then they lie on the branch (II)
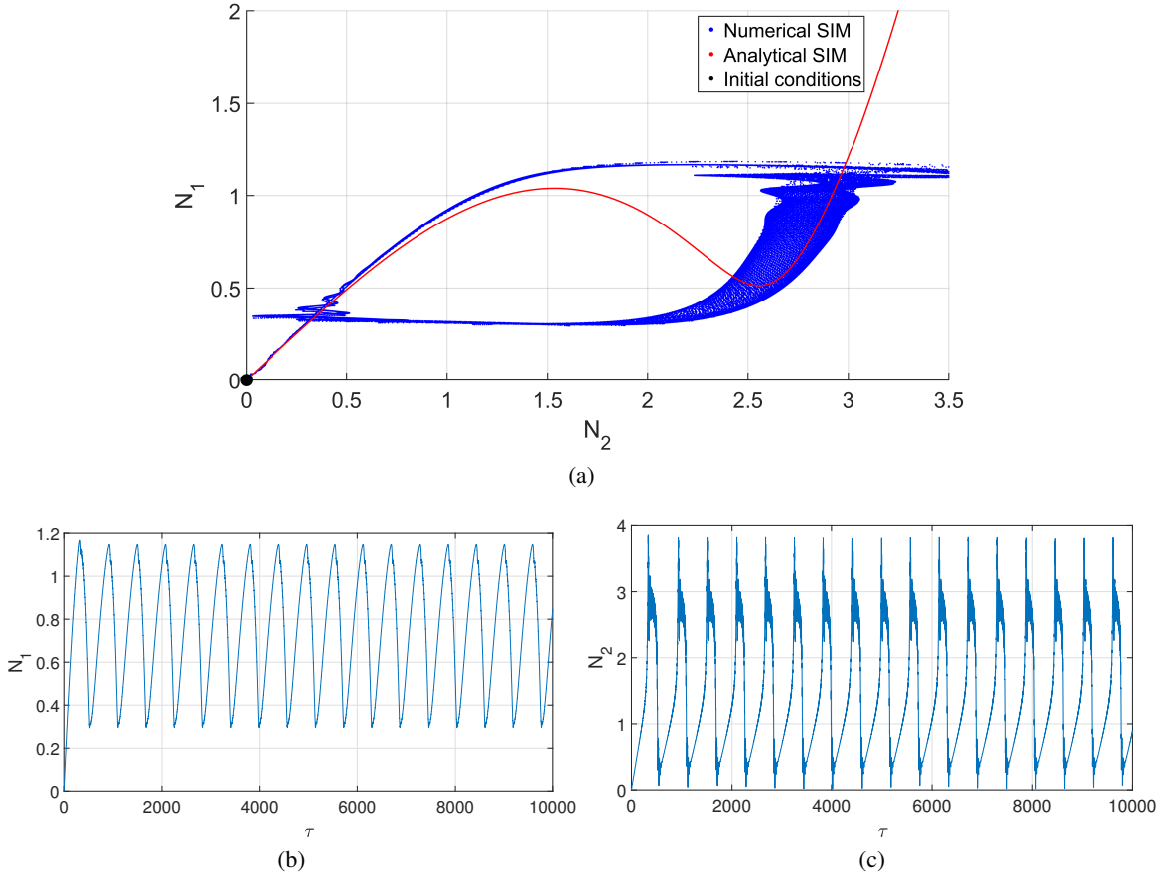
Figure 5: Analytical predictions versus numerical results for the system (with parameters of Table 2) under external excitation with $f_0 = 1.1$ and $\sigma = 1$. Numerical results are obtained by direct integration of Eq. (3) with initial conditions as $(u_1(\tau = 0), u_2(\tau = 0), u_1'(\tau = 0), u_2'(\tau = 0)) = (0, 0, 0, 0)$ (represented by a solid point ($\bullet$)). a) The SIM and corresponding numerical results; b) Time histories of N_1 obtained by numerical integration; c) Time histories of N_2 obtained by numerical integration.

of backbone curve and all types of frequency response curves of the forced system follow its backbone curve. For the design aspects, detection of backbone and frequency response curves, provide good information about possible system amplitudes as functions of the frequency and also amplitude of external excitations.
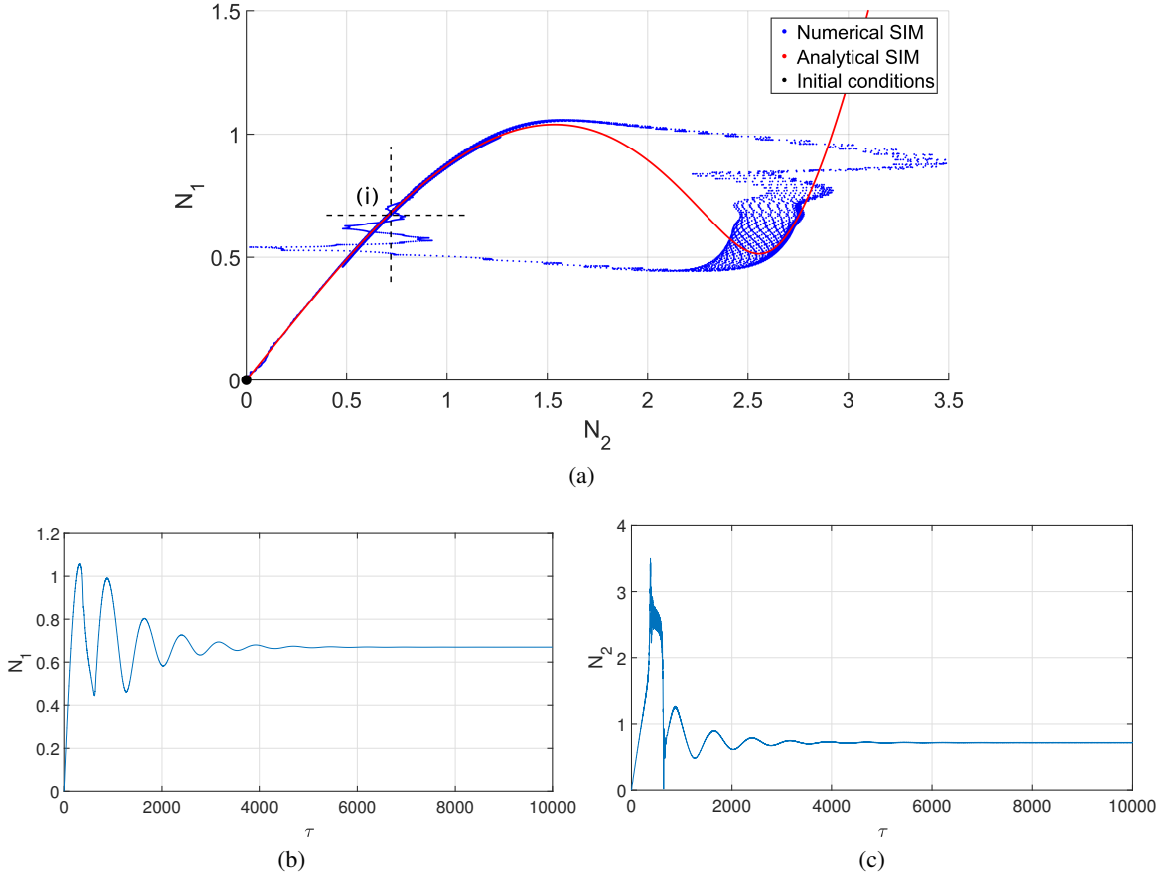
(a)

(b)

(c)

Figure 6: Analytical predictions versus numerical results for the system (with parameters of Table 2) under external excitation with $f_0 = 1.1$ and $\sigma = -0.3$. Numerical results are obtained by direct integration of Eq. (3) with initial conditions as $(u_1(\tau = 0), u_2(\tau = 0), u'_1(\tau = 0), u'_2(\tau = 0)) = (0, 0, 0, 0)$ (represented by a solid point ($\bullet$)). a) The SIM and corresponding numerical results; b) Time histories of N_1 obtained by numerical integration; c) Time histories of N_2 obtained by numerical integration. (i) is the first equilibrium point.

4 Detection of different dynamics of the system with time-dependent cubic nonlinearity

4.1 Description of the system

Here, the results of previous sections will be expanded to consider a time-dependent cubic nonlinearity for the second oscillator with the mass m. We assume that the function $\Lambda(u_2)$ in Eq. (1) and Fig. 1 reads: $\Lambda(u_2) = k_2(t)u_2^3$. After introducing the new time domain τ (see Eq. (2)), the $\varepsilon\Lambda_0(u_2)$ in Eq. (3) is defined as:

$$\varepsilon\Lambda_0(u_2) = \varepsilon k_0(\tau)u_2^3 \tag{40}$$

and all other parameters which are defined in Sect. 2.1 remain unchanged. In Eq. (40), we assume that $k_0(\tau)$ is $\dfrac{2\pi}{\nu}$ periodic around a constant value K_0. Thus, we suppose that $k_0(\tau)$ can be developed in term of Fourier series as:

$$k_0(\tau) = \sum_{n=-\infty}^{+\infty} K_n e^{in\nu\tau} \tag{41}$$
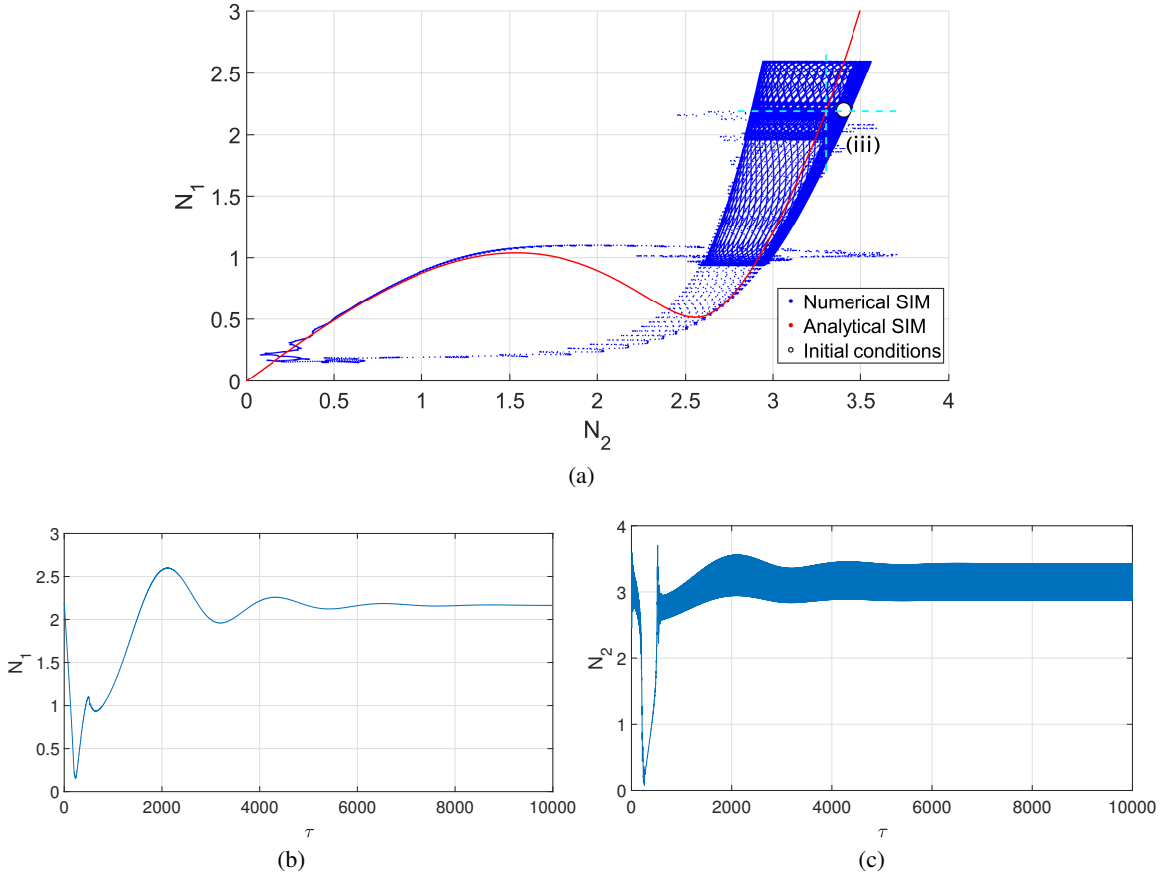
12

(a)

(b)

(c)

Figure 7: Analytical predictions versus numerical results for the system (with parameters of Table 2) under external excitation with $f_0 = 1.1$ and $\sigma = -0.3$. Numerical results are obtained by direct integration of Eq. (3) with initial conditions as $(u_1(\tau = 0), u_2(\tau = 0), u_1'(\tau = 0), u_2'(\tau = 0)) = (2.2, 3.4, 0, 0)$ (represented by a hollow circle ($\circ$)). a) The SIM and corresponding numerical results. b) Time histories of N_1 obtained by numerical integration; c) Time histories of N_2 obtained by numerical integration. (iii) is the third equilibrium point.
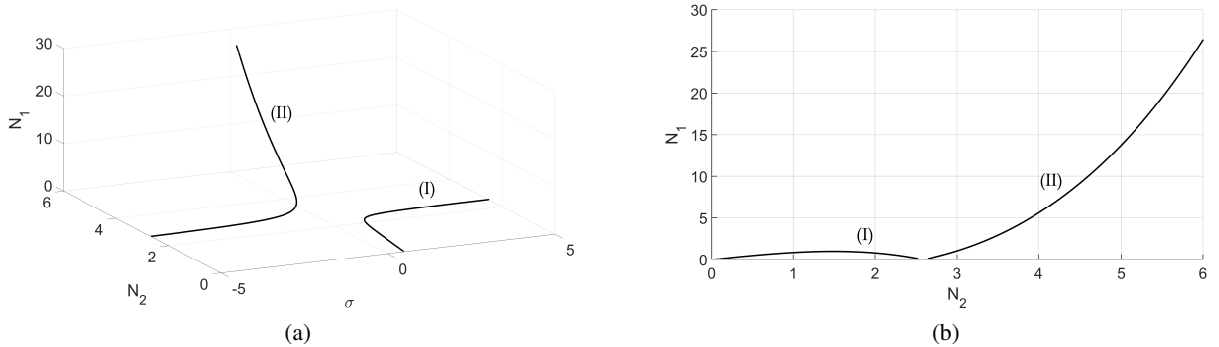

(a)

(b)

Figure 8: Backbone curve of the system with the parameters of the Table 2. The backbone curve possesses two branches, namely (I) and (II). a) Three-dimensional view (σ, N_2, N_1); b) Two-dimensional view (N_2, N_1).
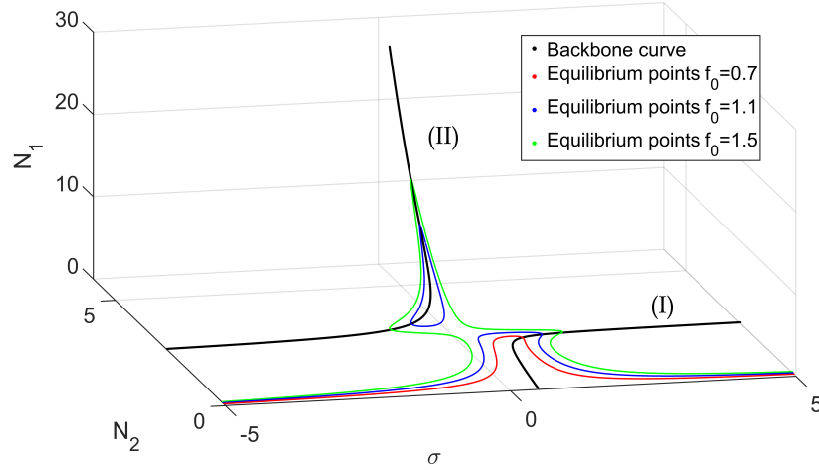
Figure 9: Backbone curves and equilibrium points of the system with different external forcing amplitudes: $f_0 = 0.7$, $f_0 = 1.1$ and $f_0 = 1.5$ (parameters of the Table 2).

4.2 Complexification of the system and applying the Galerkin method

Let us introduce the complex variables of Manevitch [35], see Eq. (4), and apply the Galerkin method to keep the first harmonics. Following system is obtained:

$$\begin{cases} \phi_1' + \dfrac{i}{2}\nu\phi_1 + \dfrac{1}{2}\varepsilon\xi_1\phi_1 + \dfrac{1}{2i\nu}\phi_1 + \varepsilon\gamma_0\dfrac{1}{2i\nu}(\phi_1 - \phi_2) = \dfrac{\varepsilon f_0}{2i} & (42.1) \\[2ex] \varepsilon(\phi_2' + \dfrac{i}{2}\nu\phi_2) + \dfrac{1}{2}\varepsilon\xi_2\phi_2 + \varepsilon\gamma_0\dfrac{1}{2i\nu}(\phi_2 - \phi_1) + \varepsilon G(u_2) = 0 & (42.2) \end{cases} \quad (42)$$

Where $G(u_2)$ is defined in Eq. (8). Applying Eq. (41) in Eq. (8), we obtain:

$$G(\phi_2, \phi_2^*) = \frac{i}{8\nu^3}\left[\phi_2^3 K_{-2} - 3K_0|\phi_2|^2\phi_2 + 3K_2|\phi_2|^2\phi_2^* - \phi_2^{*3}K_4\right] \quad (43)$$

In the following section, Eq. (42) will be considered at different orders of ε to identify the fast and slow dynamics of the system, as explained in Sect. 2.3.

4.3 Fast system dynamics

After obtaining Eq. (9), the $\mathcal{H}$ function for this case reads:

$$\mathcal{H} = \frac{1}{2}i\phi_2 + \frac{1}{2}\xi_2\phi_2 - \frac{i\gamma_0}{2}(\phi_2 - \phi_1) + \frac{i}{8}\left[\phi_2^3 K_{-2} - 3K_0|\phi_2|^2\phi_2 + 3K_2|\phi_2|^2\phi_2^* - \phi_2^{*3}K_4\right] \quad (44)$$

So equation of the SIM in complex domain becomes:

$$\phi_1 = (-1 + \gamma_0 + i\xi_2)\frac{\phi_2}{\gamma_0} - \frac{1}{4\gamma_0}\left(\phi_2^3 K_{-2} + 3|\phi_2|^2\left[-\phi_2 K_0 + \phi_2^* K_2\right] - \phi_2^{3*}K_4\right) \quad (45)$$

Where $K_0 \in \mathbb{R}$ and $K_j = K_{jR} + iK_{jI}$, $j = \{2, 4\}$. Moreover, $K_{-j} = K_j^*$. After going to polar domain (see Eq. 11), following system can be obtained:

$$N_1 = \frac{N_2}{\gamma_0}\sqrt{A^2 + B^2} \quad (46)$$

$$\delta_1 = \delta_2 + \arctan\left(\frac{B}{A}\right) \quad (47)$$

with $A(N_2, \delta_2)$ and $B(N_2, \delta_2)$ defined in Appendix B. Equation (46), reveals that for a system with a periodic time-dependent nonlinearity, the SIM becomes three-dimensional depending on N_1, N_2 and δ_2.

To detect the local extrema of the SIM and for the sake of simplicity in Eq. (46), we analyse functions $\dfrac{\partial N_1^2}{\partial N_2} = 0$ and $\dfrac{\partial N_1^2}{\partial \delta_2} = 0$, whose details are presented in Appendix C. Let us set $X = N_2^2$:

$$\begin{cases} \dfrac{\partial N_1^2}{\partial N_2} = 0 \Rightarrow \alpha_4 X^2 + \alpha_2 X + \alpha_0 = 0 \\[4mm] \dfrac{\partial N_1^2}{\partial \delta_2} = 0 \Rightarrow \beta_2 X + \beta_0 = 0 \end{cases} \tag{48}$$

Hence,

$$X = -\frac{\beta_0}{\beta_2} \tag{49}$$

By injecting Eq. (49) into Eq. (48), we obtain:

$$P(\delta_2) = \alpha_4 \beta_0^2 - \alpha_2 \beta_0 \beta_2 + \alpha_0 \beta_2^2 = 0 \tag{50}$$

Equation (50) depends only on δ_2, so the values of δ_2 which verified the equation $P(\delta_2) = 0$ can be found. Consequently, the obtained values of δ_2 correspond to local extrema of the SIM. Then, associate values of N_2 and N_1 can be calculated from Eqs. (49) and (46), respectively. The points collecting these sets of (δ_2, N_2, N_1) correspond to coordinates of local extrema of the SIM.

4.4 Unstable zones of the SIM

To determine the boundaries of the unstable zones, we are interested in Eq. (9.2) which is written as:

$$\frac{\partial \phi_2}{\partial T_0} + \frac{1}{2} \left[i\phi_2 + \xi_2 \phi_2 - i\gamma_0(\phi_2 - \phi_1) + \frac{i}{4} \left(\phi_2^3 K_2^* - 3\phi_2^2 \phi_2^* K_0 + 3\phi_2 \phi_2^{*2} K_2 - \phi_2^{*3} K_4 \right) \right] = 0 \tag{51}$$

After taking into account the complex conjugate of Eq. (51), and introducing the perturbation from of the variables (see Eq. (13)), the arrays of $\mathbb{M}$ matrix in Eq. (14), become:

$$\begin{cases} \mathbb{M}_{11} = -\dfrac{i}{2} \left(1 - \gamma_0 + \dfrac{3}{4} \left[\phi_2^2 K_2^* - 2\phi_2 \phi_2^* K_0 + \phi_2^{*2} K_2 \right] \right) - \dfrac{\xi_2}{2} \\[3mm] \mathbb{M}_{12} = -\dfrac{3i}{8} \left(-\phi_2^2 K_0 + 2\phi_2 \phi_2^* K_2 - \phi_2^{*2} K_4 \right) \\[3mm] \mathbb{M}_{21} = \dfrac{3i}{8} \left(-\phi_2^{*2} K_0 + 2\phi_2 \phi_2^* K_2^* - \phi_2^2 K_4^* \right) \\[3mm] \mathbb{M}_{22} = \dfrac{i}{2} \left(1 - \gamma_0 + \dfrac{3}{4} \left[\phi_2^{*2} K_2 - 2\phi_2 \phi_2^* K_0 + \phi_2^2 K_2^* \right] \right) - \dfrac{\xi_2}{2} \end{cases} \tag{52}$$

Eigenvalues (λ_1, λ_2) of $\mathbb{M}$ matrix can be obtained from Eq. (30). Then, α and β in Eq. (31) read:

$$\begin{cases} \alpha = -\xi_2 \\ \beta = a_v N_2^4 + b_v N_2^2 + c_v \end{cases} \tag{53}$$

with (a_v, b_v and c_v defined in Appendix D). As explained in Sect. 3.3, the condition $\beta = 0$, clarifies boundaries between stable and unstable zones of the SIM. Let us set $X = N_2^2$. If X_1 and X_2 are real and positive solutions of $\beta = 0$ in Eq. (53), then $N_{21} = \sqrt{X_1}$ and $N_{22} = \sqrt{X_2}$ correspond to boundaries of the unstable zones of the SIM.

4.5 Slow system dynamics

The $\mathbb{A}$ matrix of Eq. (17) becomes:

$$
\mathbb{A} = \frac{1}{2}
\begin{bmatrix}
i(1-\gamma_0) + \xi_2 + \dfrac{3i}{4}\left(\phi_2^2 K_2^* - 2|\phi_2|^2 K_0 + \phi_2^{*2} K_2\right) & \dfrac{i}{4}\left(-3\phi_2^2 K_0 + 6|\phi_2|^2 K_2 - 3\phi_2^{*2} K_4\right) \\
-\dfrac{i}{4}\left(-3\phi_2^{*2} K_0 + 6|\phi_2|^2 K_2^* - 3\phi_2^2 K_4^*\right) & -i(1-\gamma_0) + \xi_2 - \dfrac{3i}{4}\left(\phi_2^{*2} K_2 - 2|\phi_2|^2 K_0 + \phi_2^2 K_2^*\right)
\end{bmatrix}
\tag{54}
$$

To determine the slow dynamic of the system, we consider Eq. (42.1) at $O(\varepsilon)$ and we use the method which is explained in Sect. 2.3.3.

4.5.1 Singular points

The geometrical position of singular points corresponds to the N_2 values which verify $\det(\mathbb{A}) = 0$ as explained in Eq. (19). Let us assume that $X = N_2^2$ and after some mathematical developments, we will have (see Appendix E):

$$
\det(\mathbb{A}) = aX^2 + bX + c
\tag{55}
$$

We notice that Eq. (55) is the same equation as the one of the boundaries of the unstable zone of the SIM ($\beta = 0$ in Eq. (53)). Thus, for each δ_2, the singular points correspond to $N_{2,1} = \sqrt{X_1}$ and $N_{2,2} = \sqrt{X_2}$. Consequently, we see that the boundaries of the unstable zone coincide with the geometrical places of possible singularities. The associate N_1 are found via the SIM equation (see Eq. 46). Figure 10 shows the SIM of the system with its local extrema (pink point), the unstable zone (green line) which coincide with the geometrical places of singular points. The system parameters are defined in the Table 3. We observe that, unlike the system with constant nonlinear rigidity, some limited numbers of stability boundaries (or geometrical curves of singularities) correspond to local extrema.

Parameter	Value
K_0	0.1
K_{2R}	0.009
K_{2I}	0.009
K_{4R}	0
K_{4I}	0
ξ_2	0.1
γ_0	0.5

Table 3: Parameters of the system

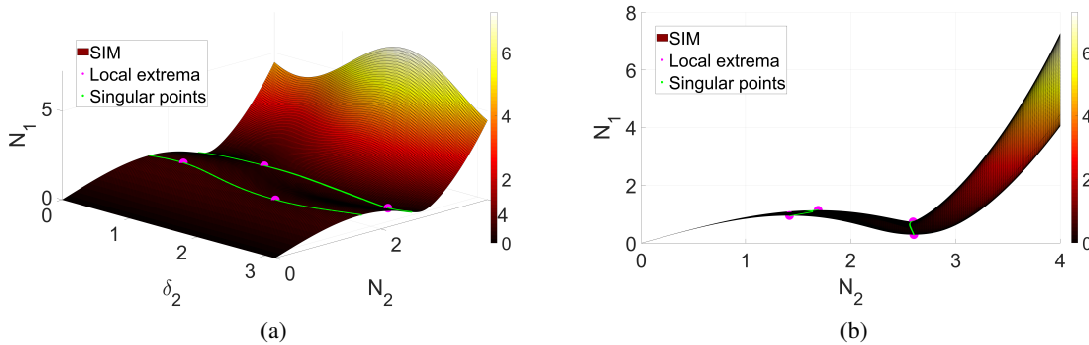(a)   (b)

Figure 10: The SIM of the system accompanied by its unstable zone (green line) and the local extrema (pink point). a) Three dimensional view (δ_2, N_2, N_1); b) Two dimensional view (N_2, N_1) (parameters of the system are provided in Table 3).

Necessary condition for having real and positive solutions of Eq. (55) leads to following conditions for damping:

$$\xi_2 \leq \xi_{2,cv} \tag{56}$$

where

$$\begin{aligned}
\xi_{2,cv} = &-(-1+\gamma_0)^2 (K_0^2 + 4K_{2I}^2 + 4K_{2R}^2 + K_{4I}^2 + K_{4R}^2 - 4(K_{2I}K_{4I} + K_{2R}(K_0 + K_{4R}))\cos(2\delta_2) \\
&+ 2K_0 K_{4R}\cos(4\delta_2) - 4(K_0 K_{2I} + K_{2R}K_{4I} - K_{2I}K_{4R})\sin(2\delta_2) + 2K_0 K_{4I}\sin(4\delta_2)) \\
&[-3K_0^2 + 2K_{2I}^2 + 2K_{2R}^2 + K_{4I}^2 + K_{4R}^2 - 4(-K_0 K_{2R} + K_{2I}K_{4I} + K_{2R}K_{4R})\cos(2\delta_2)
\end{aligned}$$
$$+2(K_{2I}^2 - K_{2R}^2 + K_0 K_{4R})\cos(4\delta_2) + 4(-K_{2R}K_{4I} + K_{2I}(K_0 + K_{4R}))\sin(2\delta_2) + 2(-2K_{2I}K_{2R} + K_0 K_{4I})\sin(4\delta_2)]^{-1} \tag{57}$$

If $\xi_2 > \xi_{2,cv}$, the SIM becomes monotone, without possessing any singularities and local extrema.

4.5.2 Detection of equilibrium points of the system

The equilibrium points correspond to $\mathcal{E} = 0$, from Eq. (15):

$$if_0 + (i(2\sigma - \gamma_0) + \xi_1)\phi_1 + i\gamma_0\phi_2 = 0 \tag{58}$$

After injecting Eq. (45) (SIM) in Eq. (58) and some mathematical manipulations, following system is obtained (see Appendix F):

$$p_{10}N_2^{10} + p_8 N_2^8 + p_7 N_2^7 + p_6 N_2^6 + p_5 N_2^5 + p_4 N_2^4 + p_3 N_2^3 + p_2 N_2^2 + p_0 = 0 \tag{59}$$

with p_j, $j = 0, ...10$ defined in Appendix F. The sets of ($\delta_2 \in \mathbb{R}$, $N_2 \in \mathbb{R}_+$ and $\sigma \in \mathbb{R}$) verifying Eq. (59) correspond to the equilibrium points of the system. The roots of Eq. (59) in term of N_2 are calculated with the "roots" function of MATLAB® for a range of given δ_2 and σ. The associate N_1 can be find via the equation of the SIM (Eq. (46)).

4.5.3 Detection of backbone curves of the system

To determine the backbone curves of the system with the time-dependent nonlinear rigidity, as in Sect. 3.5.2 we seek for periodic responses of the free and undamped system. That is to say in Eq. (58) we set $f_0 = 0$ and $\xi_1 = \xi_2 = 0$. After some mathematical manipulations, we have:

$$p_{bc,4}X^4 + p_{bc,3}X^3 + p_{bc,2}X^2 + p_{bc,1}X + p_{bc,0} = 0 \tag{60}$$

with $X = N_2^2$ and $p_{bc,j}$, $j = 0, ...4$ defined in Appendix G. As in the previous part, $X = N_2^2$ and we admit only real and positive solutions of X in Eq. (60). The associates values of N_1 can be obtained from Eq. (46).

In the next section, some numerical results will be presented. They will be considered as base results concerning the evolution of system behaviours and will be compared with the analytical predictions.

4.6 Numerical results

We consider the system parameters which are presented in Table 3. We suppose that the amplitude of external excitation is $f_0 = 1.1$. Figure 11a collects equilibrium points in terms of δ_2, N_2 and N_1 and Fig. 11b is the two-dimensional view of the Fig. 11a. Figure 11c represents the equilibrium points in terms of σ, N_2 and N_1. All of these figures are the frequency responses of the system. Figures 11d and 11e correspond to the two-dimensional views of Fig. 11c. The green part corresponds to equilibrium points which are housed by the unstable zone of the SIM. From these figures we observe that the equilibrium points are located on two global branches: a main branch (i) and isola (ii).

4.6.1 Analytical predictions versus resilts of direct numerical integrations

Some numerical integrations of the governing equations of the system (see Eq. (3)) are carried out to check the validity of obtained analytical predictions. We provide some examples for two different values of σ and different initial conditions.
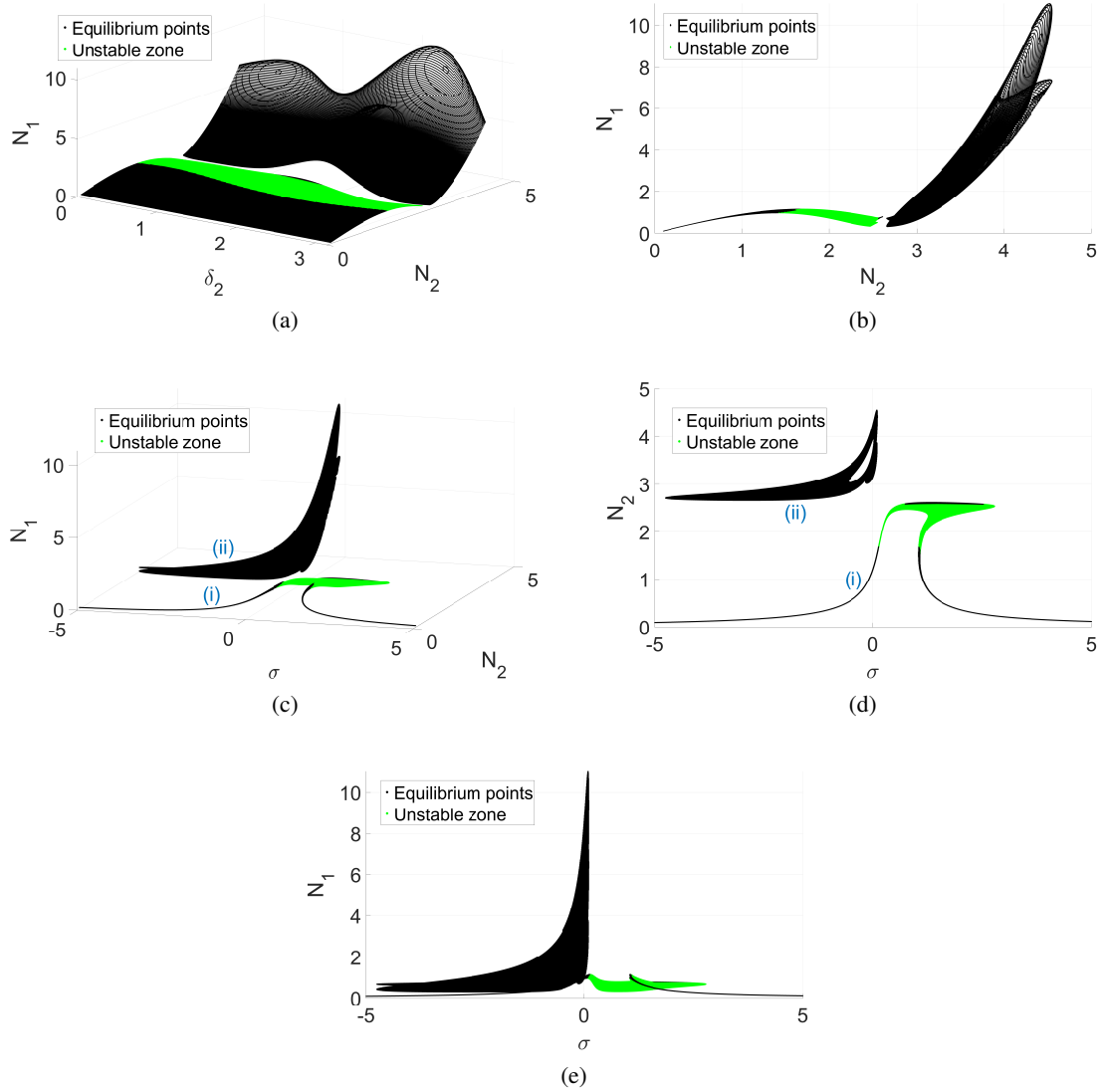
(a)

(b)

(c)

(d)

(e)

Figure 11: Different views of collected equilibrium points for the system with $f_0 = 1.1$. a) (δ_2, N_2, N_1); b) (N_2, N_1); c) (σ, N_2, N_1); d) (σ, N_2); e) (σ, N_1). The equilibrium points located in unstable zone of the SIM are represented in green.

- $\sigma = 0.5$

  For $\sigma = 0.5$, the equilibrium points are in the unstable zone of the SIM (see Fig. 11). We suppose following initial conditions: $(u_1(\tau = 0), u_2(\tau = 0), u_1'(\tau = 0), u_2'(\tau = 0)) = (0, 0, 0, 0)$. Figures 12a and 12b collect results obtained from direct numerical integration of Eq. (3) (blue line), the SIM and the initial conditions (white point). Time histories of system responses are illustrated in Figs. 12c, 12d and 12e. Figure 12 indicates that the system presents a SMR [56] which corresponds to repeated bifurcations between the stable branches of the SIM. This is because of positioning of the equilibrium point in the unstable area of the SIM.
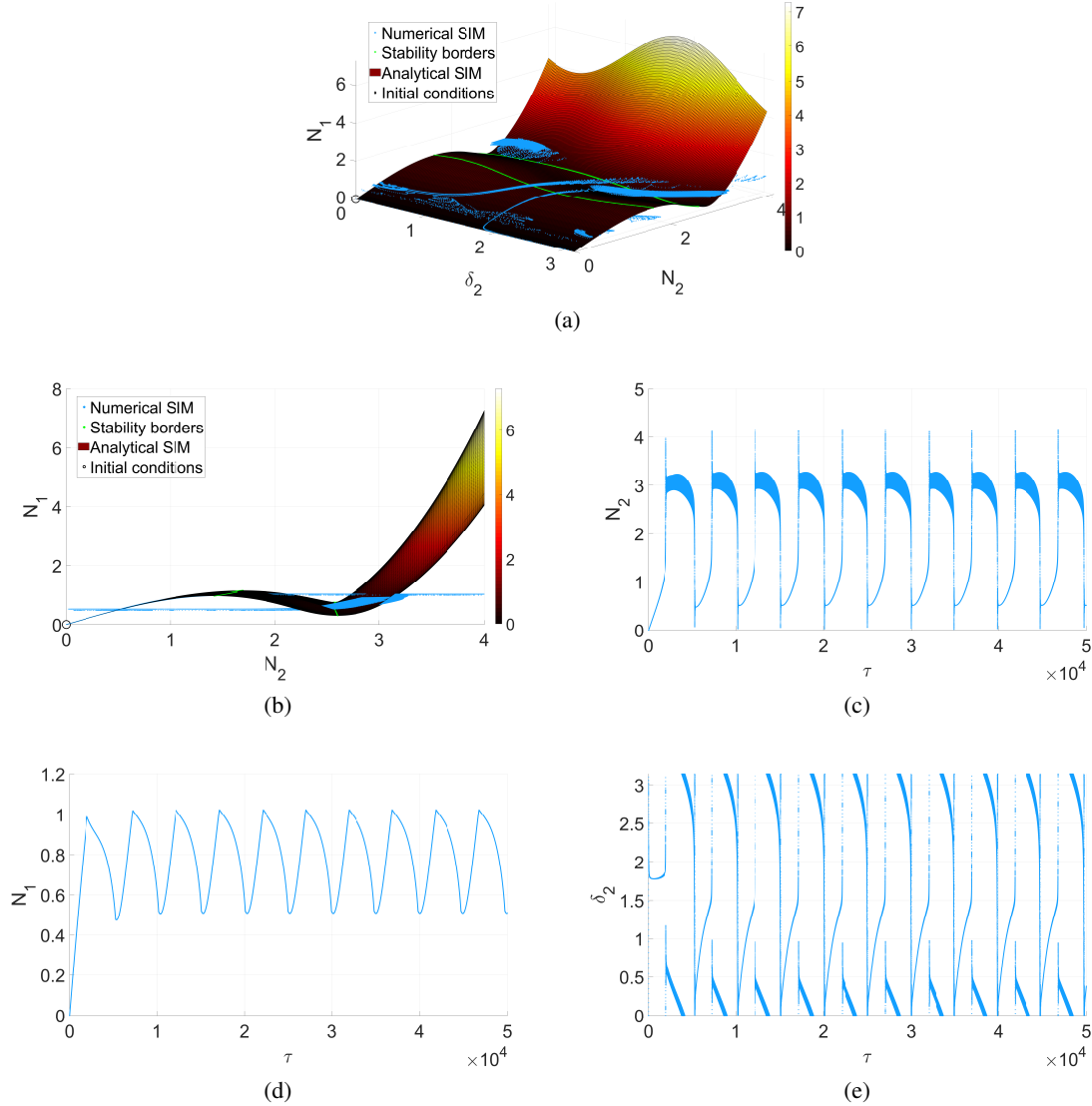
(a)

(b)

(c)

(d)

(e)

Figure 12: Analytical predictions versus numerical results for the system (with parameters of Table 3) under external excitation with $f_0 = 1.1$ and $\sigma = 0.5$. Numerical results are obtained by direct numerical integration of Eq. (3) with initial conditions as $(u_1(\tau = 0), u_2(\tau = 0), u_1'(\tau = 0), u_2'(\tau = 0)) = (0, 0, 0, 0)$ (represented by a hollow circle (○)). a) Three-dimensions view of the SIM and corresponding numerical results; b) Two-dimensions view of the SIM and corresponding numerical results; c) Time histories of N_2 obtained by numerical integration; d) Time histories of N_1 obtained by numerical integration; e) Time histories of δ_2 obtained by numerical integration. The phase δ_2 is wrapped to $[0, \pi]$.

- $\sigma = -0.56$

  For $\sigma = -0.56$, there are several equilibrium points which are located on isola (see Fig. 11). We carry out two numerical integrations with the following initial conditions:

- $(u_1(\tau = 0), u_2(\tau = 0), u_1'(\tau = 0), u_2'(\tau = 0)) = (0, 0, 0, 0)$ (see Fig. 13). The system is attracted by the main branch of frequency responses (i) (see Figs. 11c and 11d).
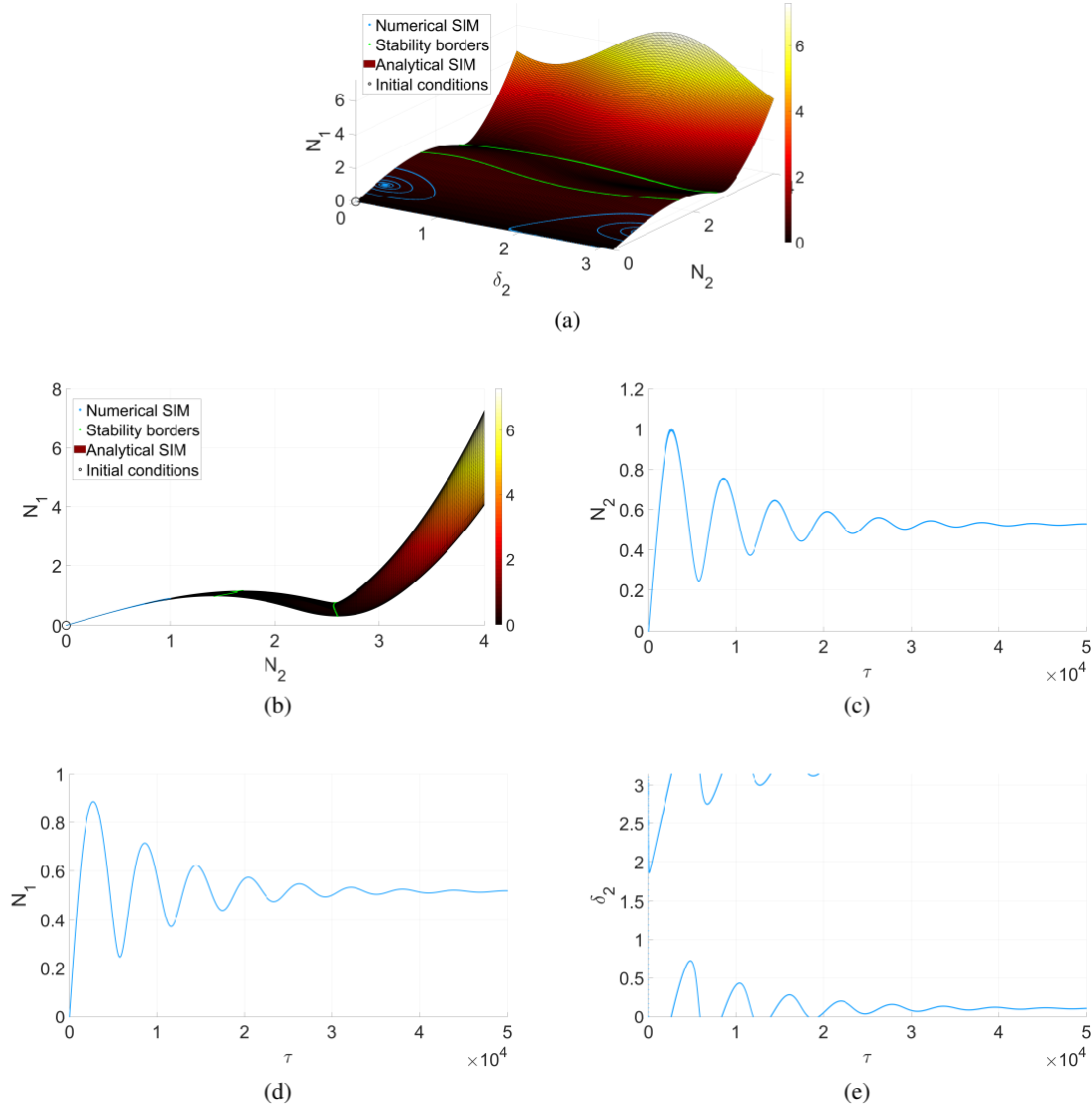
(a)

(b)

(c)

(d)

(e)

Figure 13: Analytical predictions versus numerical results for the system (with parameters of Table 3) under external excitation with $f_0 = 1.1$ and $\sigma = -0.56$. Numerical results are obtained by direct numerical integration of Eq. (3) with initial conditions as $(u_1(\tau = 0), u_2(\tau = 0), u_1'(\tau = 0), u_2'(\tau = 0)) = (0, 0, 0, 0)$ (represented by a hollow circle ($\circ$)). a) Three-dimensions view of the SIM and corresponding numerical results; b) Two-dimensions view of the SIM and corresponding numerical results; c) Time histories of N_2 obtained by numerical integration; d) Time histories of N_1 obtained by numerical integration; e) Time histories of δ_2 obtained by numerical integration. The phase δ_2 is wrapped to $[0, \pi]$.

- $(u_1(\tau = 0), u_2(\tau = 0), u_1'(\tau = 0), u_2'(\tau = 0)) = (3.5, 4, 0, 0)$ (see Fig. 14). The system is attracted by the isola of frequency responses (ii) (see Figs. 11c and 11d).

4.6.2   Backbone curve of the system

Figure 15a obtained from Eq. (60) shows the backbone curve of the system with the parameters of the Table 3 but with $\xi_1 = \xi_2 = 0$ and $f_0 = 0$. This figure collects two branches namely, (I) and (II). Figure 15b represents the two-dimensional view of the Fig. 15a. The frequency responses of the system (parameters of the Table 3) under a
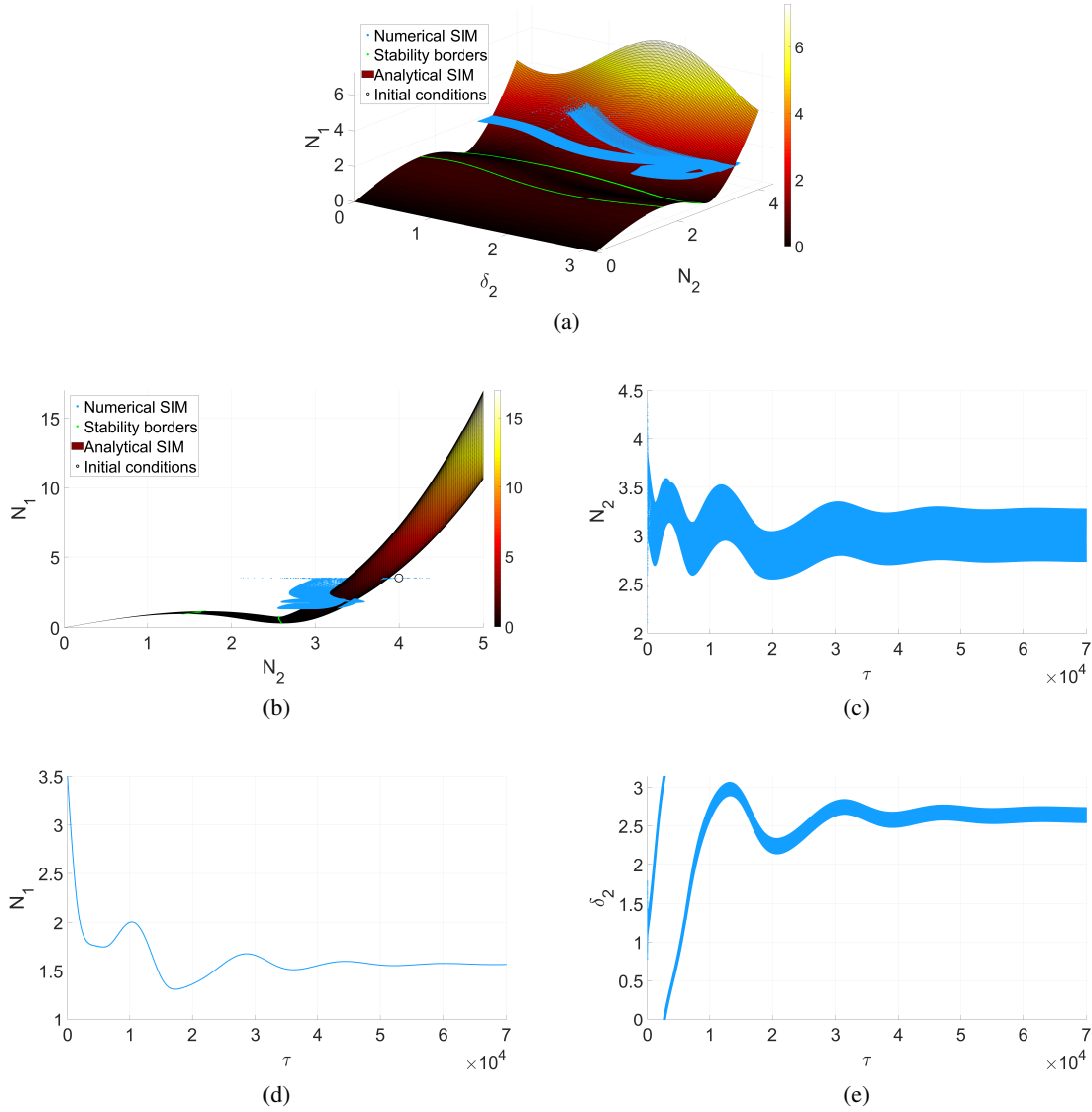
(a)

(b)

(c)

(d)

(e)

Figure 14: Analytical predictions versus numerical results for the system (with parameters of Table 3) under external excitation with $f_0 = 1.1$ and $\sigma = -0.56$. Numerical results are obtained by direct numerical integration of Eq. (3) with initial conditions as $(u_1(\tau = 0), u_2(\tau = 0), u_1'(\tau = 0), u_2'(\tau = 0)) = (3.5, 4, 0, 0)$ (represented by a hollow circle (∘)). a) Three-dimensions view of the SIM and corresponding numerical results; b) Two-dimensions view of the SIM and corresponding numerical results; c) Time histories of N_2 obtained by numerical integration; d) Time histories of N_1 obtained by numerical integration; e) Time histories of δ_2 obtained by numerical integration. The phase δ_2 is wrapped to $[0, \pi]$.

forcing amplitude $f_0 = 1.1$ are added to the backbone curve and illustrated in Fig. 16. As in Sect. 3, we can see that the backbone curve collects (almost) local maxima of the frequency response curve.
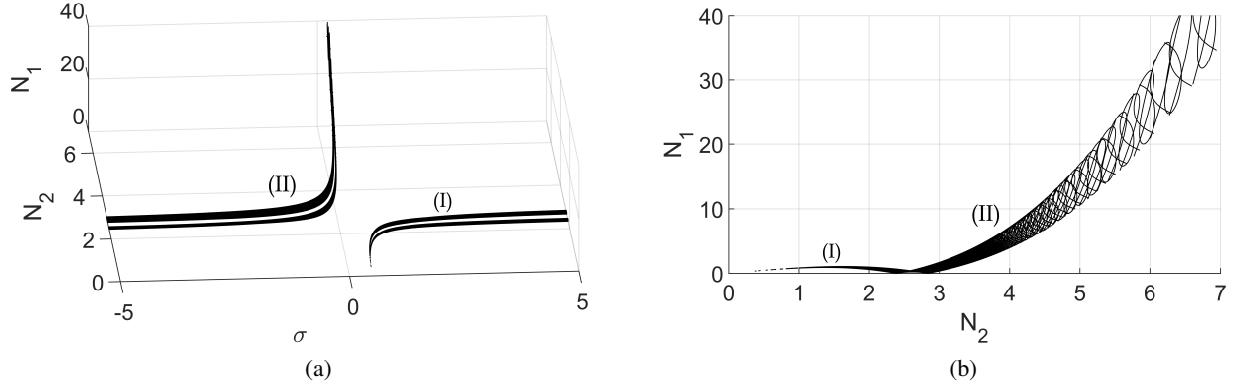

Figure 15: Backbone curve of the system with the parameters of the Table 3. The backbone curve possesses two branches, namely (I) and (II). a) Three-dimensional view (σ, N_2, N_1); b) Two-dimensional view (N_2, N_1).
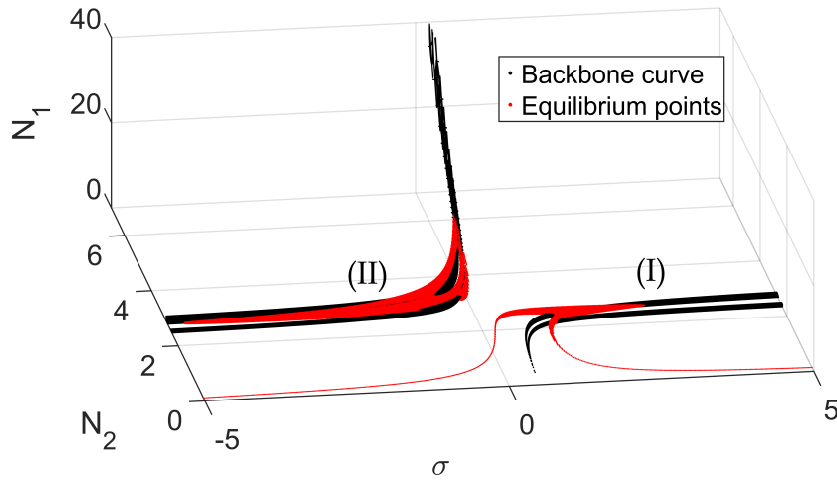

Figure 16: Backbone curves and equilibrium points of the system with the external forcing amplitude as $f_0 = 1.1$ (parameters of the Table 3).

5 Conclusions

The energy channelling between two oscillators is studied: one of oscillators supposed to be linear, is weakly coupled to a cubic nonlinear oscillator which its nonlinearity can be constant or time-dependent. Fast and slow system dynamics are detected which result in detection of slow invariant manifold of the system and its characteristic points, i.e. equilibrium and singular points. All of these, provide tools for prediction of different possible periodic or non-periodic regimes as functions of excitation amplitude and its deriving frequency. It is spotted that: i) the time-dependent nonlinearity produces a phase-dependent slow invariant manifold which its unstable zone can cover a zone of the slow invariant manifold in a continuous manner or some closed form portions of it; ii) in slow invariant manifolds of both time-dependent and constant nonlinear systems, the positions of stability borders and geometrical places of singularities coincide while positions of local extrema in time-dependent systems correspond to some few points of the stability borders; iii) the phase of the system interacts in frequency responses of time-dependent nonlinear systems and in both types of nonlinear systems, the frequency responses can present isola. The latter should be examined and identified carefully if the final goal is systems control; iv) studying frequency responses of the system permits to grasp all possible

zones of the slow invariant manifold which house equilibrium and singular points as functions of characteristics of external excitation.

The perspective of this paper could be performing stability analysis at slow time scale and also optimization of system parameters. Experimental tests will be carried out as well based on developments of this paper.

Our developments provide design tools for tuning parameters of the second oscillators for mastering energy channelling between two oscillators or all possible dynamical regimes. The system under consideration can be seen as a meta-cell which can produce special characteristics to be used later chain or a network of such cells.

Acknowledgements

Conflict of interest

The authors declare that they have no conflict of interest.

A   Treatment of $\mathcal{E} = 0$

$$\mathcal{E} = 0 \Rightarrow if_0 + [i(2\sigma - \gamma_0) + \xi_1]\phi_1 + i\gamma_0\phi_2 = 0 \tag{61}$$

Let us inject Eq. (22) in Eq. (61),

$$if_0 + [i(2\sigma - \gamma_0) + \xi_1]\frac{\phi_2}{\gamma_0}\left[-1 + i\xi_2 + \gamma_0 + \frac{3}{4}k_0|\phi_2|^2\right] + i\gamma_0\phi_2 = 0 \tag{62}$$

$$if_0 + [i(2\sigma - \gamma_0) + \xi_1]\frac{N_2 e^{i\delta_2}}{\gamma_0}\left[-1 + i\xi_2 + \gamma_0 + \frac{3}{4}k_0 N_2^2\right] + i\gamma_0 N_2 e^{i\delta_2} = 0 \tag{63}$$

$$if_0 + \frac{N_2(\cos(\delta_2) + i\sin(\delta_2))}{\gamma_0}\left[-\xi_2(2\sigma - \gamma_0) + i(2\sigma - \gamma_0)\left(-1 + \gamma_0 + \frac{3}{4}k_0 N_2^2\right)\right.$$
$$\left. + i\xi_1\xi_2 + \xi_1\left(-1 + \gamma_0 + \frac{3}{4}k_0 N_2^2\right)\right] + i\gamma_0 N_2(\cos(\delta_2) + i\sin(\delta_2)) = 0 \tag{64}$$

Real part:

$$\cos(\delta_2)\underbrace{\left[-\xi_2(2\sigma - \gamma_0) + \xi_1\left(-1 + \gamma_0 + \frac{3}{4}k_0 N_2^2\right)\right]}_{A_{11}}$$
$$- \sin(\delta_2)\underbrace{\left[(2\sigma - \gamma_0)\left(-1 + \gamma_0 + \frac{3}{4}k_0 N_2^2\right) + \xi_1\xi_2 + \gamma_0^2\right]}_{A_{12}} = 0 \tag{65}$$

Imaginary part:

$$\cos(\delta_2)\underbrace{\left[(2\sigma - \gamma_0)\left(-1 + \gamma_0 + \frac{3}{4}k_0 N_2^2\right) + \xi_1\xi_2 + \gamma_0^2\right]}_{A_{12}}$$
$$+ \sin(\delta_2)\underbrace{\left[-\xi_2(2\sigma - \gamma_0) + \xi_1\left(-1 + \gamma_0 + \frac{3}{4}k_0 N_2^2\right)\right]}_{A_{11}} = \underbrace{-\frac{f_0\gamma_0}{N_2}}_{C_2} \tag{66}$$

$$\begin{cases} A_{11}\cos(\delta_2) - A_{12}\sin(\delta_2) = 0 \\ A_{12}\cos(\delta_2) + A_{11}\sin(\delta_2) = C_2 \end{cases} \tag{67}$$

$$A_{11}^2 + A_{12}^2 = C_2^2 \tag{68}$$

$$\xi_2^2(2\sigma - \gamma_0)^2 - 2\xi_2\xi_1(2\sigma - \gamma_0)\left(-1 + \gamma_0 + \frac{3}{4}k_0 N_2^2\right) + \xi_1^2\left(-1 + \gamma_0 + \frac{3}{4}k_0 N_2^2\right)^2 + (2\sigma - \gamma_0)^2$$

$$\left(-1 + \gamma_0 + \frac{3}{4}k_0 N_2^2\right)^2 + 2(2\sigma - \gamma_0)\left(-1 + \gamma_0 + \frac{3}{4}k_0 N_2^2\right)(\xi_1\xi_2 + \gamma_0^2) + (\xi_1\xi_2 + \gamma_0^2)^2 = \frac{f_0^2\gamma_0^2}{N_2^2} \tag{69}$$

Let us consider $X = N_2^2$

$$X^3\left(\frac{3}{4}k_0\right)^2\left[\xi_1^2 + (2\sigma - \gamma_0)^2\right] + X^2\frac{3}{2}k_0\left[(-1 + \gamma_0)\left[\xi_1^2 + (2\sigma_- \gamma_0)^2\right] + (2\sigma - \gamma_0)\gamma_0^2\right]$$

$$+ X\left[(-1 + \gamma_0)^2\left[\xi_1^2 + 2(\sigma - \gamma_0)^2\right] + 2(-1 + \gamma_0)(2\sigma - \gamma_0)\gamma_0^2 + (\xi_1\xi_2 + \gamma_0^2)^2 + (2\sigma - \gamma_0)^2\xi_2^2\right] = f_0^2\gamma_0^2 \tag{70}$$

$$aX^3 + bX^2 + cX + d = 0 \tag{71}$$

B Development of fast dynamic for the system with time-dependent nonlinearity

$$\gamma_0 N_1 e^{i\delta_1} = (-1 + \gamma_0 + i\xi_2) N_2 e^{i\delta_2} - \frac{N_2^3}{4}\left(e^{3i\delta_2}(K_{2R} - iK_{2I}) + 3\left[-K_0 e^{i\delta_2} + (K_{2R} + iK_{2I}) e^{-i\delta_2}\right]\right.$$

$$\left. - (K_{4R} + iK_{4I}) e^{-i3\delta_2}\right) \tag{72}$$

Real part:

$$\gamma_0 \frac{N_1}{N_2}\cos(\delta_1 - \delta_2) = \underbrace{(-1 + \gamma_0) - \frac{N_2^2}{4}\left(4K_{2R}\cos(2\delta_2) + 4K_{2I}\sin(2\delta_2) - 3K_0 - K_{4R}\cos(4\delta_2) - K_{4I}\sin(4\delta_2)\right)}_{A}$$

$$\tag{73}$$

Imaginary part:

$$\gamma_0 \frac{N_1}{N_2}\sin(\delta_1 - \delta_2) = \underbrace{\xi_2 - \frac{N_2^2}{4}\left(-2K_{2R}\sin(2\delta_2) + 2K_{2I}\cos(2\delta_2) + K_{4R}\sin(4\delta_2) - K_{4I}\cos(4\delta_2)\right)}_{B} \tag{74}$$

So,

$$N_1 = \frac{N_2}{\gamma_0}\sqrt{A^2 + B^2} \tag{75}$$

$$A^2 + B^2 = \frac{1}{16}[16\xi_2^2 + (-8K_{4R}N_2^2\sin(4\delta_2) + 8K_{4I}N_2^2\cos(4\delta_2) + 16K_{2R}N_2^2\sin(2\delta_2)$$
$$- 16K_{2I}N_2^2\cos(2\delta_2))\xi_2 + ((-4K_{2R}K_{4R} - 8K_{2I}K_{4I})N_2^4\sin(2\delta_2) + (4K_{2I}K_{4R} - 8K_{2R}K_{4I})N_2^4\cos(2\delta_2)$$
$$+ 6K_0K_{4I}N_2^4 + (8K_{4I}\gamma_0 - 8K_{4I})N_2^2)\sin(4\delta_2) + ((4K_{2R}K_{4I} - 8K_{2I}K_{4R})N_2^4\sin(2\delta_2)$$
$$+ (-8K_{2R}K_{4R} - 4K_{2I}K_{4I})N_2^4\cos(2\delta_2) + 6K_0K_{4R}N_2^4 + (8K_{4R}\gamma_0 - 8K_{4R})N_2^2)\cos(4\delta_2)+$$
$$(24K_{2I}K_{2R}N_2^4\cos(2\delta_2) - 24K_0K_{2I}N_2^4 + (32K_{2I} - 32K_{2I}\gamma_0)N_2^2)\sin(2\delta_2) + (12K_{2R}^2$$
$$- 12K_{2I}^2)N_2^4\cos^2(2\delta_2) + ((32K_{2R} - 32K_{2R}\gamma_0)N_2^2$$
$$- 24K_0K_{2R}N_2^4)\cos(2\delta_2) + (K_{4R}^2 + K_{4I}^2 + 4K_{2R}^2 + 16K_{2I}^2 + 9K_0^2)N_2^4$$
$$+ (24K_0\gamma_0 - 24K_0)N_2^2 + 16\gamma_0^2 - 32\gamma_0 + 16] \quad (76)$$

C   Extrema of the SIM for the system with time-dependent nonlinearity

$$\frac{\partial N_1^2}{\partial N_2} = \frac{-1}{8\gamma_0^2}[((12K_{2R}K_{4R} + 24K_{2I}K_{4I})N_2^5\sin(2\delta_2) + (24K_{2R}K_{4I} - 12K_{2I}K_{4R})N_2^5\cos(2\delta_2)$$
$$- 18K_0K_{4I}N_2^5 + (16K_{4R}\xi_2 + (16 - 16\gamma_0)K_{4I})N_2^3)\sin(4\delta_2) + ((24K_{2I}K_{4R} - 12K_{2R}K_{4I})N_2^5\sin(2\delta_2)$$
$$+ (24K_{2R}K_{4R} + 12K_{2I}K_{4I})N_2^5\cos(2\delta_2) - 18K_0K_{4R}N_2^5 + ((16 - 16\gamma_0)K_{4R} - 16K_{4I}\xi_2)N_2^3)\cos(4\delta_2)$$
$$+ (-72K_{2I}K_{2R}N_2^5\cos(2\delta_2) + 72K_0K_{2I}N_2^5 + ((64\gamma_0 - 64)K_{2I} - 32K_{2R}\xi_2)N_2^3)\sin(2\delta_2) + (36K_{2I}^2$$
$$- 36K_{2R}^2)N_2^5\cos^2(2\delta_2) + (72K_0K_{2R}N_2^5 + (32K_{2I}\xi_2 + (64\gamma_0 - 64)K_{2R})N_2^3)\cos(2\delta_2)$$
$$+ (-3K_{4R}^2 - 3K_{4I}^2 - 12K_{2R}^2 - 48K_{2I}^2 - 27K_0^2)N_2^5 + (48 - 48\gamma_0)K_0N_2^3 + (-16\xi_2^2 - 16\gamma_0^2 + 32\gamma_0 - 16)N_2] = 0$$
$$(77)$$

$$\frac{\partial N_1^2}{\partial \delta_2} = \frac{1}{2\gamma_0^2}[(3K_{2I}K_{4R}N_2^6\sin(2\delta_2) + 3K_{2R}K_{4R}N_2^6\cos(2\delta_2) - 3K_0K_{4R}N_2^6$$
$$+ ((4 - 4\gamma_0)K_{4R} - 4K_{4I}\xi_2)N_2^4)\sin(4\delta_2) + (-3K_{2I}K_{4I}N_2^6\sin(2\delta_2) - 3K_{2R}K_{4I}N_2^6\cos(2\delta_2)$$
$$+ 3K_0K_{4I}N_2^6 + ((4\gamma_0 - 4)K_{4I} - 4K_{4R}\xi_2)N_2^4)\cos(4\delta_2) + ((6K_{2I}^2$$
$$- 6K_{2R}^2)N_2^6\cos(2\delta_2) + 6K_0K_{2R}N_2^6 + (4K_{2I}\xi_2 + (8\gamma_0 - 8)K_{2R})N_2^4)\sin(2\delta_2) + 12K_{2I}K_{2R}N_2^6\cos^2(2\delta_2)$$
$$+ ((4K_{2R}\xi_2 + (8 - 8\gamma_0)K_{2I})N_2^4 - 6K_0K_{2I}N_2^6)\cos(2\delta_2) - 6K_{2I}K_{2R}N_2^6] = 0 \quad (78)$$

Eq. (77) and (78) read as a polynomial of N_2.

$$\frac{N_2}{8\gamma_0^2}(16 - 32\gamma_0 + 16\gamma_0^2 + 16\xi_2^2) + \frac{N_2^3}{8\gamma_0^2}(48K_0(-1 + \gamma_0) + 64K_{2R}\cos(2\delta_2) - 64K_{2R}\gamma_0\cos(2\delta_2)$$
$$- 32K_{2I}\xi_2\cos(2\delta_2) - 16K_{4R}\cos(4\delta_2) + 16K_{4R}\gamma_0\cos(4\delta_2) + 16K_{4I}\xi_2\cos(4\delta_2) + 64K_{2I}\sin(2\delta_2)$$
$$- 64K_{2I}\gamma_0\sin(2\delta_2) + 32K_{2R}\xi_2\sin(2\delta_2) - 16K_{4I}\sin(4\delta_2) + 16K_{4I}\gamma_0\sin(4\delta_2) - 16K_{4R}\xi_2\sin(4\delta_2))$$
$$+ \frac{N_2^5}{8\gamma_0^2}(27K_0^2 + 30K_{2I}^2 + 30K_{2R}^2 + 3K_{4I}^2 + 3K_{4R}^2 - 72K_0K_{2R}\cos(2\delta_2) - 18K_{2I}K_{4I}\cos(2\delta_2)$$
$$- 18K_{2R}K_{4R}\cos(2\delta_2) - 18K_{2I}^2\cos(4\delta_2) + 18K_{2R}^2\cos(4\delta_2) + 18K_0K_{4R}\cos(4\delta_2) + 6K_{2I}K_{4I}\cos(6\delta_2)$$
$$- 6K_{2R}K_{4R}\cos(6\delta_2) - 72K_0K_{2I}\sin(2\delta_2) - 18K_{2R}K_{4I}\sin(2\delta_2) + 18K_{2I}K_{4R}\sin(2\delta_2)$$
$$+ 36K_{2I}K_{2R}\sin(4\delta_2) + 18K_0K_{4I}\sin(4\delta_2) - 6K_{2R}K_{4I}\sin(6\delta_2) - 6K_{2I}K_{4R}\sin(6\delta_2)) = 0 \quad (79)$$

25

Detection of different dynamics of two coupled oscillators including
a time-dependent cubic nonlinearity
A PREPRINT

$$\frac{N_2^4}{8\gamma_0^2}(-32K_{2I}(-1+\gamma_0)\cos(2\delta_2)+16K_{2R}\xi_2\cos(2\delta_2)-16K_{4I}\cos(4\delta_2)+16K_{4I}\gamma_0\cos(4\delta_2)$$

$$-16K_{4R}\xi_2\cos(4\delta_2)+32K_{2R}(-1+\gamma_0)\sin(2\delta_2)+16K_{2I}\xi_2\sin(2\delta_2)+16K_{4R}\sin(4\delta_2)-16K_{4R}\gamma_0\sin(4\delta_2)$$

$$-16K_{4I}\xi_2\sin(4\delta_2))+\frac{N_2^6}{8\gamma_0^2}(-6K_{2R}K_{4I}\cos(2\delta_2)+6K_{2I}(-4K_0+K_{4R})\cos(2\delta_2)+24K_{2I}K_{2R}\cos(4\delta_2)$$

$$+12K_0K_{4I}\cos(4\delta_2)-6(K_{2R}K_{4I}+K_{2I}K_{4R})\cos(6\delta_2)+6K_{2I}K_{4I}\sin(2\delta_2)+6K_{2R}(4K_0+K_{4R})\sin(2\delta_2)$$

$$+12(K_{2I}-K_{2R})(K_{2I}+K_{2R})\sin(4\delta_2)-12K_0K_{4R}\sin(4\delta_2)-6(K_{2I}K_{4I}-K_{2R}K_{4R})\sin(6\delta_2))=0 \quad (80)$$

Setting $X=N_2^2$, then Eq. (79) can be written as is simplified:

$$\frac{\partial N_1^2}{\partial N_2}=0\Rightarrow\alpha_4 X^2+\alpha_2 X+\alpha_0=0 \tag{81}$$

with

$$\alpha_0=16(1-2\gamma_0+\gamma_0^2+\xi_2^2) \tag{82}$$

$$\alpha_2=48K_0(-1+\gamma_0)+64K_{2R}\cos(2\delta_2)-64K_{2R}\gamma_0\cos(2\delta_2)-32K_{2I}\xi_2\cos(2\delta_2)-16K_{4R}\cos(4\delta_2)$$
$$+16K_{4R}\gamma_0\cos(4\delta_2)+16K_{4I}\xi_2\cos(4\delta_2)+64K_{2I}\sin(2\delta_2)-64K_{2I}\gamma_0\sin(2\delta_2)+32K_{2R}\xi_2\sin(2\delta_2)-16K_{4I}\sin(4\delta_2)$$
$$+16K_{4I}\gamma_0\sin(4\delta_2)-16K_{4R}\xi_2\sin(4\delta_2) \tag{83}$$

$$\alpha_4=27K_0^2+30K_{2I}^2+30K_{2R}^2+3K_{4I}^2+3K_{4R}^2-72K_0K_{2R}\cos(2\delta_2)-18K_{2I}K_{4I}\cos(2\delta_2)-18K_{2R}K_{4R}\cos(2\delta_2)$$
$$-18K_{2I}^2\cos(4\delta_2)+18K_{2R}^2\cos(4\delta_2)+18K_0K_{4R}\cos(4\delta_2)+6K_{2I}K_{4I}\cos(6\delta_2)-6K_{2R}K_{4R}\cos(6\delta_2)$$
$$-72K_0K_{2I}\sin(2\delta_2)-18K_{2R}K_{4I}\sin(2\delta_2)+18K_{2I}K_{4R}\sin(2\delta_2)+36K_{2I}K_{2R}\sin(4\delta_2)+18K_0K_{4I}\sin(4\delta_2)$$
$$-6K_{2R}K_{4I}\sin(6\delta_2)-6K_{2I}K_{4R}\sin(6\delta_2) \tag{84}$$

Equation (80) can be written as:

$$\frac{\partial N_1^2}{\partial\delta_2}=0\Rightarrow\beta_2 X+\beta_0=0 \tag{85}$$

with

$$\beta_0=-32K_{2I}(-1+\gamma_0)\cos(2\delta_2)+16K_{2R}\xi_2\cos(2\delta_2)-16K_{4I}\cos(4\delta_2)+16K_{4I}\gamma_0\cos(4\delta_2)-16K_{4R}\xi_2\cos(4\delta_2)$$
$$+32K_{2R}(-1+\gamma_0)\sin(2\delta_2)+16K_{2I}\xi_2\sin(2\delta_2)+16K_{4R}\sin(4\delta_2)-16K_{4R}\gamma_0\sin(4\delta_2)-16K_{4I}\xi_2\sin(4\delta_2)$$
$$\tag{86}$$

$$\beta_2=-6K_{2R}K_{4I}\cos(2\delta_2)+6K_{2I}(-4K_0+K_{4R})\cos(2\delta_2)+24K_{2I}K_{2R}\cos(4\delta_2)+12K_0K_{4I}\cos(4\delta_2)$$
$$-6(K_{2R}K_{4I}+K_{2I}K_{4R})\cos(6\delta_2)+6K_{2I}K_{4I}\sin(2\delta_2)+6K_{2R}(4K_0+K_{4R})\sin(2\delta_2)$$
$$+12(K_{2I}-K_{2R})(K_{2I}+K_{2R})\sin(4\delta_2)-12K_0K_{4R}\sin(4\delta_2)-6(K_{2I}K_{4I}-K_{2R}K_{4R})\sin(6\delta_2) \tag{87}$$

D   Development unstable zone of the SIM of the system with time-dependent nonlinearity

$$a_v=\frac{9}{64}(3K_0^2-2K_{2I}^2-2K_{2R}^2-K_{4I}^2-K_{4R}^2+4(-K_0K_{2R}+K_{2I}K_{4I}+K_{2R}K_{4R})\cos(2\delta_2)$$
$$-2(K_{2I}^2-K_{2R}^2+K_0K_{4R})\cos(4\delta_2)-4(-K_{2R}K_{4I}+K_{2I}(K_0+K_{4R}))\sin(2\delta_2)+2(2K_{2I}K_{2R}-K_0K_{4I})\sin(4\delta_2)) \tag{88}$$

$$b_v = \frac{3}{4} \left(-1 + \gamma_0 \right) \left(K_0 - K_{2R} \cos(2\delta_2) - K_{2I} \sin(2\delta_2) \right) \tag{89}$$

$$c_v = \frac{1}{4} \left((-1 + \gamma_0)^2 + \xi_2^2 \right) \tag{90}$$

E   Development of $\det(\mathbb{A})$ (singular points of the system with time-dependent nonlinearity)

$$\det(\mathbb{A}) = \frac{\partial \mathscr{H}}{\partial \phi_2} \frac{\partial \mathscr{H}^*}{\partial \phi_2^*} - \frac{\partial \mathscr{H}^*}{\partial \phi_2} \frac{\partial \mathscr{H}}{\partial \phi_2^*} \tag{91}$$

$$\det(\mathbb{A}) = \frac{1}{4} \left[\xi_2^2 + \left(-1 + \gamma_0 - \frac{3}{4} \left(\phi_2^2 K_2^* - 2|\phi_2|^2 K_0 + \phi_2^{*2} K_2 \right) \right)^2 - \left(\frac{3}{4} \right)^2 \left(|\phi_2|^4 - 2|\phi_2|^2 \phi_2^{*2} K_0 K_2 \right. \right.$$
$$+ \phi_2^{*4} K_0 K_4 - 2|\phi_2|^2 \phi_2^2 K_0 K_2^* + 4|\phi_2|^4 |K_2|^2$$
$$\left. \left. - 2|\phi_2|^2 \phi_2^{*2} K_2^* K_4 + \phi_2^4 K_0 K_4^* - 2|\phi_2|^2 \phi_2^2 K_2 K_4^* + |\phi_2|^4 |K_4|^2 \right) \right] \tag{92}$$

$$\det(\mathbb{A}) = \frac{1}{4} [\xi_2^2 + (-1 + \gamma_0)^2 - 3(-1 + \gamma_0) N_2^2 (K_{2R} \cos(2\delta_2) + K_{2I} \sin(2\delta_2) - K_0)$$
$$+ \frac{9}{4} N_2^4 (K_{2R} \cos(2\delta_2) + K_{2I} \sin(2\delta_2) - K_0)^2 - N_2^4 (\frac{3}{4})^2 (K_0^2 - 4K_0(K_{2R} \cos(2\delta_2) + K_{2I} \sin(2\delta_2))$$
$$+ 2K_0(K_{4R} \cos(4\delta_2) + K_{4I} \sin(4\delta_2)) - 4(K_{2R} K_{4R} \cos(2\delta_2) - K_{2I} K_{4R} \sin(2\delta_2)$$
$$+ K_{4I} K_{2I} \cos(2\delta_2) + K_{2R} K_{4I} \sin(2\delta_2)) + 4(K_{2R}^2 + K_{2I}^2) + K_{4R}^2 + K_{4I}^2)] \tag{93}$$

$$\det(\mathbb{A}) = a N_2^4 + b N_2^2 + c \tag{94}$$

Let us consider $X = N_2^2$:

$$\det(\mathbb{A}) = \frac{1}{4} \left(aX^2 + bX + c \right) \tag{95}$$

with

$$a = \frac{-1}{64} [18K_0 K_{4I} \sin(4\delta_2) + 18K_0 K_{4R} \cos(4\delta_2) + (-72K_{2I} K_{2r} \cos(2\delta_2) + 36K_{2I} K_{4R} - 36K_{2R} K_{4I}$$
$$+ 36K_0 K_{2I}) \sin(2\delta_2) + (36K_{2I}^2 - 36K_{2R}^2) \cos(2\delta_2)^2 + (-36K_{2R} K_{4R} - 36K_{2I} K_{4I} + 36K_0 K_{2R}) \cos(2\delta_2)$$
$$+ 9K_{4R}^2 + 9K_{4I}^2 + 36K_{2R}^2 - 27K_0^2] \tag{96}$$

$$b = \frac{-3}{4} \left(-1 + \gamma_0 \right) \left(K_{2R} \cos(2\delta_2) + K_{2I} \sin(2\delta_2) - K_0 \right) \tag{97}$$

$$c = \frac{\xi_2^2}{4} \left(-1 + \gamma_0 \right)^2 \tag{98}$$

27

F   Development of equilibrium points of the system with time-dependent nonlinearity

$$if_0 + (i(2\sigma - \gamma_0) + \xi_1)\phi_1 + i\gamma_0\phi_2 = 0 \tag{99}$$

Injecting Eq. (45) in Eq. (99):

$$if_0 + (i(2\sigma - \gamma_0) + \xi_1)\frac{1}{\gamma_0}(-1 + \gamma_0 + i\xi_2)\phi_2 - \frac{1}{4}\left(\phi_2^3 K_2^* - 3|\phi_2|^2\phi_2 K_0 + 3|\phi_2|^2\phi_2^* K_2 - \phi_2^{*3}K_4\right) + i\gamma_0\phi_2 = 0 \tag{100}$$

$$if_0 + (i(2\sigma - \gamma_0) + \xi_1)\frac{N_2 e^{i\delta_2}}{\gamma_0}\left[-1 + \gamma_0 + i\xi_2 - \frac{N_2^2}{4}\left(K_2^* e^{2i\delta_2} - 3K_0 + 3e^{-2i\delta_2}K_2 - e^{-4i\delta_2}K_4\right)\right]$$
$$+ i\gamma_0 N_2 e^{i\delta_2} = 0 \quad (101)$$

Real part:

$$N_2((3\gamma_0 K_{2I}N_2^2 - 6K_{2I}N_2^2\sigma + 4\xi_1 - 4\gamma_0\xi_1 - 3K_0 N_2^2\xi_1 + 3K_{2R}N_2^2\xi_1 - 4\gamma_0\xi_2 + 8\sigma\xi_2)\cos(\delta_2)$$
$$+ (-\gamma_0 K_{2I}N_2^2 - \gamma_0 K_{4I}N_2^2 + 2K_{2I}N_2^2\sigma + 2K_{4I}N_2^2\sigma + K_{2R}N_2^2\xi_1 - K_{4R}N_2^2\xi_1)\cos(3\delta_2) + (4\gamma_0$$
$$- 3\gamma_0 K_0 N_2^2 - 3\gamma_0 K_{2R}N_2^2 - 8\sigma + 8\gamma_0\sigma + 6K_0 N_2^2\sigma + 6K_{2R}N_2^2\sigma + 3K_{2I}N_2^2\xi_1 + 4\xi_1\xi_2)\sin(\delta_2)$$
$$+ (\gamma_0 K_{2R}N_2^2 + \gamma_0 K_{4R}N_2^2 - 2K_{2R}N_2^2\sigma - 2K_{4R}N_2^2\sigma + K_{2I}N_2^2\xi_1 - K_{4I}N_2^2\xi_1)\sin(3\delta_2)) \quad (102)$$

Imaginary part:

$$4f_0\gamma_0 + (4\gamma_0 N_2 - 3\gamma_0 K_0 N_2^3 + 3\gamma_0 K_{2R}N_2^3 - 8N_2\sigma + 8\gamma_0 N_2\sigma + 6K_0 N_2^3\sigma - 6K_{2R}N_2^3\sigma$$
$$- 3K_{2I}N_2^3\xi_1 + 4N_2\xi_1\xi_2)\cos(\delta_2) + (\gamma_0 K_{2R}N_2^3 - \gamma_0 K_{4R}N_2^3 - 2K_{2R}N_2^3\sigma + 2K_{4R}N_2^3\sigma + K_{2I}N2^3\xi_1$$
$$+ K_{4I}N_2^3\xi_1)\cos(3\delta_2) + (3\gamma_0 K_{2I}N_2^3 - 6K_{2I}N_2^3\sigma - 4N_2\xi_1 + 4\gamma_0 N_2\xi_1 + 3K_0 N_2^3\xi_1 + 3K_{2R}N_2^3\xi_1 + 4\gamma_0 N_2\xi_2$$
$$- 8N_2\sigma\xi_2)\sin(\delta_2) + (\gamma_0 K_{2I}N_2^3 - \gamma_0 K_{4I}N_2^3 - 2K_{2I}N_2^3\sigma + 2K_{4I}N_2^3\sigma - K_{2R}N_2^3\xi_1 - K_{4R}N_2^3\xi_1)\sin(3\delta_2)$$
$$(103)$$

Hence,

$$\begin{cases} a_1\cos(\delta_2) + b_1\sin(\delta_2) = c_1 \\ a_2\cos(\delta_2) + b_2\sin(\delta_2) = c_2 \end{cases} \tag{104}$$

with

$$\begin{cases} a_1 = (3\gamma_0 K_{2I}N_2^2 - 6K_{2I}N_2^2\sigma + 4\xi_1 - 4\gamma_0\xi_1 - 3K_0 N_2^2\xi_1 + 3K_{2R}N_2^2\xi_1 - 4\gamma_0\xi_2 + 8\sigma\xi_2) \\ b_1 = (4\gamma_0 - 3\gamma_0 K_0 N_2^2 - 3\gamma_0 K_{2R}N_2^2 - 8\sigma + 8\gamma_0\sigma + 6K_0 N_2^2\sigma + 6K_{2R}N_2^2\sigma + 3K_{2I}N_2^2\xi_1 + 4\xi_1\xi_2) \\ c_1 = -((-\gamma_0 K_{2I}N_2^2 - \gamma_0 K_{4I}N_2^2 + 2K_{2I}N_2^2\sigma + 2K_{4I}N_2^2\sigma + K_{2R}N_2^2\xi_1 - K_{4R}N_2^2\xi_1)\cos(3\delta_2) \\ \quad + (\gamma_0 K_{2R}N_2^2 + \gamma_0 K_{4R}N_2^2 - 2K_{2R}N_2^2\sigma - 2K_{4R}N_2^2\sigma + K_{2I}N_2^2\xi_1 - K_{4I}N_2^2\xi_1)\sin(3\delta_2)) \\ a_2 = (4\gamma_0 N_2 - 3\gamma_0 K_0 N_2^3 + 3\gamma_0 K_{2R}N_2^3 - 8N_2\sigma + 8\gamma_0 N_2\sigma + 6K_0 N_2^3\sigma - 6K_{2R}N_2^3\sigma \\ \quad - 3K_{2I}N_2^3\xi_1 + 4N_2\xi_1\xi_2) \\ b_2 = (3\gamma_0 K_{2I}N_2^3 - 6K_{2I}N_2^3\sigma - 4N_2\xi_1 + 4\gamma_0 N_2\xi_1 + 3K_0 N_2^3\xi_1 + 3K_{2R}N_2^3\xi_1 + 4\gamma_0 N_2\xi_2 - 8N_2\sigma\xi_2) \\ c_2 = -(4f_0\gamma_0 + (\gamma_0 K_{2R}N_2^3 - \gamma_0 K_{4R}N_2^3 - 2K_{2R}N_2^3\sigma + 2K_{4R}N_2^3\sigma + K_{2I}N_2^3\xi_1 + \\ \quad K_{4I}N_2^3\xi_1)\cos(3\delta_2) + (\gamma_0 K_{2I}N_2^3 - \gamma_0 K_{4I}N_2^3 - 2K_{2I}N_2^3\sigma + 2K_{4I}N_2^3\sigma - K_{2R}N_2^3\xi_1 \\ \quad - K_{4R}N_2^3\xi_1)\sin(3\delta_2)) \end{cases} \tag{105}$$

So,

$$(b_2 c_1 - b_1 c_2)^2 + (a_2 c_1 - a_1 c_2)^2 - (-a_2 b_1 + a_1 b_2)^2 = 0 \tag{106}$$

Equation (106) can be reorganised as a polynomial of N_2:

$$p_{10}N_2^{10} + p_8 N_2^8 + p_7 N_2^7 + p_6 N_2^6 + p_5 N_2^5 + p_4 N_2^4 + p_3 N_2^3 + p_2 N_2^2 + p_0 = 0 \tag{107}$$

Detection of different dynamics of two coupled oscillators including
a time-dependent cubic nonlinearity
A PREPRINT

with

$$
\begin{aligned}
p_{10} = -9((\gamma_0 - 2\sigma)^2 + \xi_1^2)^2 (9K_0^4 + K_0(8K_{2I}K_{2R}K_{4I} - 4K_{2I}^2 K_{4R} + 4K_{2R}^2 K_{4R}) + \\
(K_{2I}^2 + K_{2R}^2)(8K_{2I}^2 + 8K_{2R}^2 - K_{4I}^2 - K_{4R}^2) - K_0^2(19K_{2I}^2 + 19K_{2R}^2 + K_{4I}^2 + K_{4R}^2) \\
- 2(K_0^2(K_{2I}K_{4I} - K_{2R}K_{4R}) + (K_{2I}^2 + K_{2R}^2)(K_{2I}K_{4I} - K_{2R}K_{4R}) + K_0(-3K_{2I}^2 \\
K_{2R} + K_{2R}^3 - K_{2R}K_{4I}^2 + 2K_{2I}K_{4I}K_{4R} + K_{2R}K_{4R}^2))\cos(6\delta_2) + 2(K_0^2(K_{2R}K_{4I} + K_{2I}K_{4R}) \\
+ (K_{2I}^2 + K_{2R}^2)(K_{2R}K_{4I} + K_{2I}K_{4R}) + K_0(K_{2I}^3 - 2K_{2R}K_{4I}K_{4R} + K_{2I}(-3K_{2R}^2 - K_{4I}^2 + K_{4R}^2)))\sin(6\delta_2)
\end{aligned}
$$
(108)

$$
\begin{aligned}
p_8 = 24((\gamma_0 - 2\sigma)^2 + \xi_1^2)(\gamma_0(-(18K_0^3 + 4K_{2I}K_{2R}K_{4I} - 2K_{2I}^2 K_{4R} + 2K_{2R}^2 K_{4R} \\
- K_0(19K_{2I}^2 + 19K_{2R}^2 + K_{4I}^2 + K_{4R}^2))(4\sigma(1+\sigma) + \xi_1^2) - 8(K_{2I}^2 K_{4I} - K_{2R}^2 K_{4I} \\
+ 2K_{2I}K_{2R}K_{4R})\sigma\xi_2) + (4\sigma^2 + \xi_1^2)(18K_0^3 - K_0(19K_{2I}^2 + 19K_{2R}^2 + K_{4I}^2 + K_{4R}^2) - 2K_{2I}^2 \\
(K_{4R} - K_{4I}\xi_2) + 2K_{2R}^2(K_{4R} - K_{4I}\xi_2) + 4K_{2I}K_{2R}(K_{4I} + K_{4R}\xi_2)) + \gamma_0^2(18K_0^3(1+2\sigma) \\
- K_0(19K_{2I}^2 + 19K_{2R}^2 + K_{4I}^2 + K_{4R}^2)(1+2\sigma) + 2K_{2R}^2(K_{4R} + 2K_{4R}\sigma - K_{4I}(\xi_1 + \xi_2)) \\
+ 2K_{2I}^2(-K_{4R}(1+2\sigma) + K_{4I}(\xi_1 + \xi_2)) + 4K_{2I}K_{2R}(K_{4I} + 2K_{4I}\sigma + K_{4R}(\xi_1 + \xi_2))) \\
+ (\gamma_0(-(3K_{2I}^2 K_{2R} - 2K_{2I}K_{4I}(K_0 + K_{4R}) - K_{2R}(K_{2R}^2 - K_{4I}^2 - 2K_0 K_{4R} + K_{4R}^2))(4\sigma(1+\sigma) + \xi_1^2) \\
- 4(K_{2I}^3 + 2K_{2R}K_{4I}K_{4R} + K_{2I}(-3K_{2R}^2 + K_{4I}^2 - K_{4R}^2))\sigma\xi_2) + (4\sigma^2 + \xi_1^2)(3K_{2I}^2 K_{2R} - 2K_{2I}K_{4I}(K_0 + K_{4R}) \\
+ K_{2I}^3\xi_2 + K_{2I}(-3K_{2R}^2 + K_{4I}^2 - K_{4R}^2)\xi_2 + K_{2R}(-K_{2R}^2 + K_{4I}^2 + 2K_0 K_{4R} - K_{4R}^2 + 2K_{4I}K_{4R}\xi_2)) \\
+ \gamma_0^2(3K_{2I}^2(K_{2R} + 2K_{2R}\sigma) + K_{2I}^3(\xi_1 + \xi_2) + K_{2R}(-K_{2R}^2(1+2\sigma) + K_{4I}^2(1+2\sigma) - K_{4R}(-2K_0 + K_{4R}) \\
(1+2\sigma) + 2K_{4I}K_{4R}(\xi_1 + \xi_2)) - K_{2I}(2K_0(K_{4I} + 2K_{4I}\sigma) + 2K_{4I}(K_{4R} + 2K_{4R}\sigma) - K_{4I}^2(\xi_1 + \xi_2) \\
+ (3K_{2R}^2 + K_{4R}^2)(\xi_1 + \xi_2))))\cos(6\delta_2) + (-\gamma_0((K_{2I}^3 + 2K_{2R}K_{4I}(K_0 - K_{4R}) + K_{2I}(-3K_{2R}^2 - K_{4I}^2 \\
+ 2K_0 K_{4R} + K_{4R}^2))(4\sigma(1+\sigma) + \xi_1^2) + 4(-3K_{2I}^2 K_{2R} - 2K_{2I}K_{4I}K_{4R} + K_{2R}(K_{2R}^2 + K_{4I}^2 - K_{4R}^2))\sigma\xi_2) \\
+ \gamma_0^2(K_{2I}^3(1+2\sigma) - 3K_{2I}^2 K_{2R}(\xi_1 + \xi_2) - K_{2I}(K_{4I}^2(1+2\sigma) - K_{4R}(2K_0 + K_{4R})(1+2\sigma) + K_{2R}^2(3+6\sigma) \\
+ 2K_{4I}K_{4R}(\xi_1 + \xi_2)) + K_{2R}(2K_0(K_{4I} + 2K_{4I}\sigma) - 2K_{4I}(K_{4R} + 2K_{4R}\sigma) + K_{4I}^2(\xi_1 + \xi_2) + (K_{2R} - K_{4R}) \\
(K_{2R} + K_{4R})(\xi_1 + \xi_2))) + (4\sigma^2 + \xi_1^2)(K_{2I}^3 + 2K_{2R}K_{4I}(K_0 - K_{4R}) - 3K_{2I}^2 K_{2R}\xi_2 + K_{2R}(K_{2R}^2 \\
+ K_{4I}^2 - K_{4R}^2)\xi_2 + K_{2I}(-3K_{2R}^2 + K_{4R}(2K_0 + K_{4R}) - K_{4I}(K_{4I} + 2K_{4R}\xi_2))))\sin(6\delta_2)
\end{aligned}
$$
(109)

$$
\begin{aligned}
p_7 = 72 f_0 \gamma_0((\gamma_0 - 2\sigma)^2 + \xi_1^2)(((K_0^2(K_{2R} - K_{4R}) + (K_{2I}^2 + K_{2R}^2)(K_{2R} - K_{4R}) \\
- 2K_0(K_{2I}(K_{2I} + K_{4I}) + K_{2R}(-K_{2R} + K_{4R})))(\gamma_0 - 2\sigma) + (K_0^2(K_{2I} + K_{4I}) \\
+ (K_{2I}^2 + K_{2R}^2)(K_{2I} + K_{4I}) - 2K_0 K_{2R}(2K_{2I} + K_{4I}) + 2K_0 K_{2I}K_{4R})\xi_1)\cos(3\delta_2) \\
+ ((K_0^2(K_{2I} - K_{4I}) + (K_{2I}^2 + K_{2R}^2)(K_{2I} - K_{4I}) - 2K_0 K_{2R}K_{4I} + 2K_0 K_{2I}(2K_{2R} + K_{4R}))(\gamma_0 - 2\sigma) \\
- (2K_0 K_{2I}(K_{2I} - K_{4I}) + K_0^2(K_{2R} + K_{4R}) - 2K_0 K_{2R}(K_{2R} + K_{4R}) + (K_{2I}^2 + K_{2R}^2)(K_{2R} + K_{4R}))\xi_1)\sin(3\delta_2)
\end{aligned}
$$
(110)

Detection of different dynamics of two coupled oscillators including
a time-dependent cubic nonlinearity
A PREPRINT

$$p_6 = -16(\gamma_0^2(-(-54K_0^2 + 19K_{2I}^2 + 19K_{2R}^2 + K_{4I}^2 + K_{4R}^2)(8\sigma^2(3 + 2\sigma(3 + \sigma)) + 2(1 + 6\sigma + 4\sigma^2)\xi_1^2 + \xi_1^4)$$
$$- 2(-18K_0^2 + 19K_{2I}^2 + 19K_{2R}^2 + K_{4I}^2 + K_{4R}^2)\xi_1(4\sigma^2 + \xi_1^2)\xi_2 - 2(-18K_0^2 + 19K_{2I}^2 + 19K_{2R}^2 + K_{4I}^2 + K_{4R}^2)$$
$$(12\sigma^2 + \xi_1^2)\xi_2^2) + (4\sigma^2 + \xi_1^2)^2(-(19K_{2I}^2 + 19K_{2R}^2 + K_{4I}^2 + K_{4R}^2)(1 + \xi_2^2) + 18K_0^2(3 + \xi_2^2)) +$$
$$2\gamma_0^3((19K_{2I}^2 + 19K_{2R}^2 + K_{4I}^2 + K_{4R}^2)((1 + 2\sigma)(4\sigma(1 + \sigma) + \xi_1^2) + 4\sigma\xi_1\xi_2 + 4\sigma\xi_2^2) - 18K_0^2(3(1 + 2\sigma)$$
$$(4\sigma(1 + \sigma) + \xi_1^2) + 4\sigma\xi_1\xi_2 + 4\sigma\xi_2^2)) + \gamma_0^4(-(19K_{2I}^2 + 19K_{2R}^2 + K_{4I}^2 + K_{4R}^2)(1 + 4\sigma(1 + \sigma) + (\xi_1 + \xi_2)^2)$$
$$+ 18K_0^2(3 + 12\sigma(1 + \sigma) + (\xi_1 + \xi_2)^2)) - 2\gamma_0(4\sigma^2 + \xi_1^2)(-(19K_{2I}^2 + 19K_{2R}^2 + K_{4I}^2 + K_{4R}^2)(\xi_1^2 + 4\sigma(1 + \sigma + \xi_2^2))$$
$$+ 18K_0^2(3\xi_1^2 + 4\sigma(3 + 3\sigma + \xi_2^2))) - 2((\gamma_0 - 2\sigma)^2 + \xi_1^2)((4\sigma^2 + \xi_1^2)(1 + \xi_2^2) + \gamma_0^2(1 + 4\sigma(1 + \sigma) + (\xi_1 + \xi_2)^2)$$
$$- 2\gamma_0(\xi_1^2 + 2\sigma(1 + 2\sigma + \xi_2^2)))((K_{2I}K_{4I} - K_{2R}K_{4R})\cos(6\delta_2]) - (K_{2R}K_{4I} + K_{2I}K_{4R})\sin(6\delta_2))) \quad (111)$$

$$p_5 = 192f_0\gamma_0((\gamma_0^3(K_{2I}^2(1 + 2\sigma) - K_0(K_{2R} - K_{4R})(1 + 2\sigma) - K_{2R}(K_{2R} - K_{4R} + 2K_{2R}\sigma$$
$$- 2K_{4R}\sigma + K_{4I}(\xi_1 + \xi_2)) + K_{2I}(K_{4I} + 2K_{4I}\sigma - (2K_{2R} - K_{4R})(\xi_1 + \xi_2)))$$
$$- (4\sigma^2 + \xi_1^2)(K_0(-2K_{2R}\sigma + 2K_{4R}\sigma + K_{4I}\xi_1) + K_{2I}^2(2\sigma - \xi_1\xi_2) - K_{2R}(2K_{2R}\sigma$$
$$- 2K_{4R}\sigma + K_{4I}\xi_1 + 2K_{4I}\sigma\xi_2 - K_{2R}\xi_1\xi_2 + K_{4R}\xi_1\xi_2) + K_{2I}((K_0 - 2K_{2R} + K_{4R})\xi_1 + 2(-2K_{2R} + K_{4R})\sigma\xi_2$$
$$+ K_{4I}(2\sigma - \xi_1\xi_2))) - \gamma_0^2(K_0(-2(K_{2R} - K_{4R})\sigma(3 + 4\sigma) + K_{4I}\xi_1 + 2K_{4I}\sigma\xi_1 + (-K_{2R} + K_{4R})\xi_1^2)$$
$$+ K_{2I}^2(6\sigma + 8\sigma^2 - \xi_1\xi_2) - K_{2R}(2(K_{2R} - K_{4R})\sigma(3 + 4\sigma) + K_{4I}\xi_1 + 4K_{4I}\sigma\xi_1 + 6K_{4I}\sigma\xi_2$$
$$+ (-K_{2R} + K_{4R})\xi_1\xi_2) + K_{2I}(K_0(\xi_1 + 2\sigma\xi_1) - (2K_{2R} - K_{4R})(\xi_1 + 4\sigma\xi_1 + 6\sigma\xi_2) + K_{4I}(6\sigma + 8\sigma^2 - \xi_1\xi_2)))$$
$$+ \gamma_0(K_0(-4(K_{2R} - K_{4R})\sigma^2(3 + 2\sigma) + 4K_{4I}\sigma(1 + \sigma)\xi_1 - (K_{2R} - K_{4R})(1 + 2\sigma)\xi_1^2 + K_{4I}\xi_1^3)$$
$$+ K_{2I}^2(\xi_1^2 + 2\sigma(6\sigma + 4\sigma^2 + \xi_1(\xi_1 - 2\xi_2))) + K_{2I}((K_0 - 2K_{2R} + K_{4R})\xi_1(4\sigma(1 + \sigma) + \xi_1^2)$$
$$+ K_{4I}(\xi_1^2 + 2\sigma(6\sigma + 4\sigma^2 + \xi_1(\xi_1 - 2\xi_2))) - (2K_{2R} - K_{4R})(12\sigma^2 + \xi_1^2)\xi_2)$$
$$- K_{2R}(K_{2R}(\xi_1^2 + 2\sigma(6\sigma + 4\sigma^2 + \xi_1(\xi_1 - 2\xi_2))) - K_{4R}(\xi_1^2 + 2\sigma(6\sigma + 4\sigma^2 + \xi_1(\xi_1 - 2\xi_2)))$$
$$+ K_{4I}(4\sigma\xi_1 + \xi_1^2(\xi_1 + \xi_2) + 4\sigma^2(\xi_1 + 3\xi_2)))))\cos(3\delta_2) + (\gamma_0^3(-K_0(K_{2I} - K_{4I})(1 + 2\sigma) - K_{2I}^2(\xi_1 + \xi_2)$$
$$- K_{2I}(K_{4R} + 2(K_{2R} + 2K_{2R}\sigma + K_{4R}\sigma) - K_{4I}(\xi_1 + \xi_2)) + K_{2R}(K_{4I} + 2K_{4I}\sigma + (K_{2R} + K_{4R})(\xi_1 + \xi_2)))$$
$$+ (4\sigma^2 + \xi_1^2)(2K_0(K_{2I} - K_{4I})\sigma + K_0(K_{2R} + K_{4R})\xi_1 + K_{2I}^2(\xi_1 + 2\sigma\xi_2) + K_{2I}(4K_{2R}\sigma + 2K_{4R}\sigma - K_{4I}\xi_1$$
$$- (2K_{4I}\sigma + (2K_{2R} + K_{4R})\xi_1)\xi_2) - K_{2R}((K_{2R} + K_{4R})(\xi_1 + 2\sigma\xi_2) + K_{4I}(2\sigma - \xi_1\xi_2)))$$
$$+ \gamma_0^2(K_0(2(K_{2I} - K_{4I})\sigma(3 + 4\sigma) + (K_{2R} + K_{4R})(1 + 2\sigma)\xi_1 + (K_{2I} - K_{4I})\xi_1^2) + K_{2I}^2(\xi_1 + 4\sigma\xi_1 + 6\sigma\xi_2)$$
$$+ K_{2I}(2(2K_{2R} + K_{4R})\sigma(3 + 4\sigma) - K_{4I}\xi_1 - 4K_{4I}\sigma\xi_1 - (6K_{4I}\sigma + (2K_{2R} + K_{4R})\xi_1)\xi_2)$$
$$- K_{2R}((K_{2R} + K_{4R})(\xi_1 + 4\sigma\xi_1 + 6\sigma\xi_2) + K_{4I}(6\sigma + 8\sigma^2 - \xi_1\xi_2))) + \gamma_0(K_0(-4(K_{2I} - K_{4I})\sigma^2(3 + 2\sigma)$$
$$- 4(K_{2R} + K_{4R})\sigma(1 + \sigma)\xi_1 - (K_{2I} - K_{4I})(1 + 2\sigma)\xi_1^2 - (K_{2R} + K_{4R})\xi_1^3) + K_{2I}(-4(2K_{2R} + K_{4R})\sigma^2(3 + 2\sigma)$$
$$+ 4K_{4I}\sigma(1 + \sigma)\xi_1 - (2K_{2R} + K_{4R})(1 + 2\sigma)\xi_1^2 + K_{4I}\xi_1^3 + 4(2K_{2R} + K_{4R})\sigma\xi_1\xi_2 + K_{4I}(12\sigma^2 + \xi_1^2)\xi_2)$$
$$- K_{2I}^2(4\sigma\xi_1 + \xi_1^2(\xi_1 + \xi_2) + 4\sigma^2(\xi_1 + 3\xi_2)) + K_{2R}(K_{4I}(\xi_1^2 + 2\sigma(6\sigma + 4\sigma^2 + \xi_1(\xi_1 - 2\xi_2)))$$
$$+ (K_{2R} + K_{4R})(4\sigma\xi_1 + \xi_1^2(\xi_1 + \xi_2) + 4\sigma^2(\xi_1 + 3\xi_2))))))\sin(3\delta_2) \quad (112)$$

$$p_4 = -128(2(4\sigma^2 + \xi_1^2)^2(1 + \xi_2^2)^2 - 8\gamma_0(4\sigma^2 + \xi_1^2)(1 + \xi_2^2)(\xi_1^2 + 2\sigma(1 + 2\sigma + \xi_2^2)) + \gamma_0^4(3f_0^2(K_0 + K_{2R}$$
$$+ 2(K_0 + K_{2R})\sigma + K_{2I}(\xi_1 + \xi_2)) + 2(1 + 4\sigma(1 + \sigma) + (\xi_1 + \xi_2)^2)^2) + \gamma_0^2(192\sigma^3(1 + \xi_2^2) + 64\sigma^4(3 + \xi_2^2)$$
$$+ 12\sigma\xi_1(f_0^2(K_{2I} - K_{2R}\xi_2) + 4\xi_1(1 + \xi_2^2)) + 4\sigma^2(3f_0^2(K_0 + K_{2R} + K_{2I}\xi_2) + 12(1 + \xi_2^2)^2 + 8\xi_1^2(3 + \xi_2^2) + 8\xi_1(\xi_2 + \xi_2^3))$$
$$+ \xi_1^2(4 + 12\xi_1^2 + 3f_0^2(K_0 - K_{2R} - K_{2I}\xi_2) + 4\xi_2(\xi_1 + \xi_2)(2 + \xi_2(\xi_1 + \xi_2)))) - \gamma_0^3(128\sigma^4 + 64\sigma^3(3 + \xi_2^2)$$
$$+ 4\sigma^2(3f_0^2(K_0 + K_{2R}) + 8(3 + 2\xi_1^2 + 2\xi_1\xi_2 + 3\xi_2^2)) + \xi_1(8\xi_1(1 + (\xi_1 + \xi_2)^2) + 3f_0^2(2K_{2I} + K_0\xi_1 - K_{2R}(\xi_1 + 2\xi_2)))$$
$$+ 4\sigma(3f_0^2(K_0 + K_{2R} + K_{2I}(\xi_1 + \xi_2)) + 4((1 + \xi_2^2)^2 + \xi_1^2(3 + \xi_2^2) + 2\xi_1(\xi_2 + \xi_2^3)))))) \quad (113)$$

30

$$p_3 = 128 f_0 \gamma_0 ((4\sigma^2 + \xi_1^2)(1 + \xi_2^2) + \gamma_0^2(1 + 4\sigma(1 + \sigma) + (\xi_1 + \xi_2)^2) - 2\gamma_0(\xi_1^2 + 2\sigma(1 + 2\sigma + \xi_2^2)))$$
$$(((K_{2R} - K_{4R})(\gamma_0 - 2\sigma) + (K_{2I} + K_{4I})\xi_1)\cos(3\delta_2) + ((K_{2I} - K_{4I})(\gamma_0 - 2\sigma) - (K_{2R} + K_{4R}\xi_1)\sin(3\delta_2))$$
$$\tag{114}$$

$$p_2 = -128(2(4\sigma^2 + \xi_1^2)^2(1 + \xi_2^2)^2 - 8\gamma_0(4\sigma^2 + \xi_1^2)(\xi_2^2)(\xi_1^2 + 2\sigma(1 + 2\sigma + \xi_2^2))$$
$$+ \gamma_0^4(3f_0^2(K_0 + K_{2R} + 2(K_0 + K_{2R})\sigma + K_{2I}(\xi_1 + \xi_2)) + 2(1 + 4\sigma(1 + \sigma) + (\xi_1 + \xi_2)^2)^2)$$
$$+ \gamma_0^2(192\sigma^3(1 + \xi_2^2) + 64\sigma^4(3 + \xi_2^2) + 12\sigma\xi_1(f_0^2(K_{2I} - K_{2R}\xi_2) + 4\xi_1(1 + \xi_2^2)) + 4\sigma^2(3f_0^2(K_0 + K_{2R} + K_{2I}\xi_2)$$
$$+ 12(1 + \xi_2^2)^2 + 8\xi_1^2(3 + \xi_2^2) + 8\xi_1(\xi_2 + \xi_2^3)) + \xi_1^2(4 + 12\xi_1^2 + 3f_0^2(K_0 - K_{2R} - K_{2I}\xi_2) + 4\xi_2(\xi_1 + \xi_2)(2 + \xi_2(\xi_1 + \xi_2)))))$$
$$- \gamma_0^3(128\sigma^4 + 64\sigma^3(3 + \xi_2^2) + 4\sigma^2(3f_0^2(K_0 + K_{2R}) + 8(3 + 2\xi_1^2 + 2\xi_1\xi_2 + 3\xi_2^2)) + \xi_1(8\xi_1(1 + (\xi_1 + \xi_2)^2)$$
$$+ 3f_0^2(2K_{2I} + K_0\xi_1 - K_{2R}(\xi_1 + 2\xi_2))) + 4\sigma(3f_0^2(K_0 + K_{2R} + K_{2I}(\xi_1 + \xi_2)) + 4((1 + \xi_2^2)^2 + \xi_1^2(3 + \xi_2^2) + 2\xi_1(\xi_2 + \xi_2^3)))))$$
$$\tag{115}$$

$$p_0 = 256 f_0^2 \gamma_0^2 ((4\sigma^2 + \xi_1^2)(1 + \xi_2^2) + \gamma_0^2(1 + 4\sigma(1 + \sigma) + (\xi_1 + \xi_2)^2) - 2\gamma_0(\xi_1^2 + 2\sigma(1 + 2\sigma + \xi_2^2))) \tag{116}$$

G Development backbone curve with variable rigidity

$$p_{bc,0} = -256(\gamma_0 + 2(-1 + \gamma_0)\sigma)^4 \tag{117}$$

$$p_{bc,1} = 768 K_0(\gamma_0 - 2\sigma)(\gamma_0 + 2(-1 + \gamma_0)\sigma)^3 \tag{118}$$

$$p_{bc,2} = -16(\gamma_0 - 2\sigma)^2(\gamma_0 + 2(-1 + \gamma_0)\sigma)^2(54K_0^2 - 19K_{2I}^2 - 19K_{2R}^2 - K_{4I}^2 - K_{4R}^2$$
$$+ (-2K_{2I}K_{4I} + 2K_{2R}K_{4R})\cos(6\delta_2) + 2(K_{2R}K_{4I} + K_{2I}K_{4R})\sin(6\delta_2)) \tag{119}$$

$$p_{bc,3} = 24(\gamma_0 - 2\sigma)^3(\gamma_0 + 2((-1) + \gamma_0)\sigma)(18K_0^3 + 4K_{2I}K_{2R}K_{4I} - 2K_{2I}^2 K_{4R} + 2K_{2R}^2 K_{4R} - K_0(19K_{2I}^2$$
$$+ 19K_{2R}^2 + K_{4I}^2 + K_{4R}^2) + (3K_{2I}^2 K_{2R} - 2K_{2I}K_{4I}(K_0 + K_{4R}) - K_{2R}(K_{2R}^2 - K_{4I}^2 - 2K_0 K_{4R} + K_{4R}^2))\cos(6\delta_2)$$
$$+ (K_{2I}^3 + 2K_{2R}K_{4I}(K_0 - K_{4R}) + K_{2I}(-3K_{2R}^2 - K_{4I}^2 + 2K_0 K_{4R} + K_{4R}^2))\sin(6\delta_2)) \tag{120}$$

$$p_{cb,4} = -9(\gamma_0 - 2\sigma)^4(9K_0^4 + K_0(8K_{2I}K_{2R}K_{4I} - 4K_{2I}^2 K_{4R} + 4K_{2R}^2 K_{4R}) + (K_{2I}^2 + K_{2R}^2)(8K_{2I}^2 + 8K_{2R}^2 - K_{4I}^2$$
$$- K_{4R}^2) - K_0^2(19K_{2I}^2 + 19K_{2R}^2 + K_{4I}^2 + K_{4R}^2) - 2(K_0^2(K_{2I}K_{4I} - K_{2R}K_{4R}) + (K_{2I}^2 + K_{2R}^2)(K_{2I}K_{4I} - K_{2R}K_{4R})$$
$$+ K_0(-3K_{2I}^2 K_{2R} + K_{2R}^3 - K_{2R}K_{4I}^2 + 2K_{2I}K_{4I}K_{4R} + K_{2R}K_{4R}^2))\cos(6\delta_2) + 2(K_0^2 K_{2R}K_{4I} + K_{2I}K_{4R})$$
$$+ (K_{2I}^2 + K_{2R}^2)(K_{2R}K_{4I} + K_{2I}K_{4R}) + K_0(K_{2I}^3 - 2K_{2R}K_{4I}K_{4R} + K_{2I}(-3K_{2R}^2 - K_{4I}^2 + K_{4R}^2)))\sin(6\delta_2) \tag{121}$$

References

[1] G.W. Housner, L.A. Bergman, T.K. Caughey, A.G. Chassiakos, R.O. Claus, S.F. Masri, R.E. Skelton, T.T. Soong, B.F. Spencer, and J.T.P. Yao. Structural control: past, present and future. *Journal of Engineering Mechanics*, 123:897–971, 1997.

[2] S. Korkmaz. A review of active structural control: challenges for engineering informatics. *Computers and Structures*, 89:2113–2132, 2011.

[3] S.Y. Chu, T.T. Soong, and A.M. Reinhorn. *Active, Hybrid, and Semi-active Structural Control: A Design and Implementation Handbook*. Wiley, United Kingdoms, 2005.

[4] Y. Liu, T.P. Waters, and M.J. Brennan. A comparison of semi-active damping control strategies for vibration isolation of harmonic disturbances. *Journal of Sound and Vibration*, 280(1):21–39, 2005.

[5] Y. Liu, H. Matsuhisa, and H. Utsuno. Semi-active vibration isolation system with variable stiffness and damping control. *Journal of Sound and Vibration*, 313(1):16–28, 2008.

[6] S.R. Moheimani and A.J. Fleming. *Piezoelectric transducers for vibration control and damping*. Springer Science & Business Media, 2006.

[7] D. Guyomar and A. Badel. Nonlinear semi-passive multimodal vibration damping: An efficient probabilistic approach. *Journal of sound and vibration*, 294(1-2):249–268, 2006.

[8] D. Guyomar, C. Richard, and S. Mohammadi. Semi-passive random vibration control based on statistics. *Journal of Sound and Vibration*, 307(3-5):818–833, 2007.

[9] S. Mohammadi. *Semi-passive vibration control using shunted piezoelectric materials*. PhD thesis, Electronic, Electrotechnic and Automatic (EEA), INSA-Lyon, Lyon, n° 2008-ISAL-0043, 2008.

[10] V. Guillot, A. Givois, M. Colin, O. Thomas, A. Ture Savadkoohi, and C.-H. Lamarque. Theoretical and experimental investigation of a 1:3 internal resonance in a beam with piezoelectric patches. *Journal of Vibration and Control*, 26(13-14):1119–1132, 2020.

[11] V. Guillot, A. Ture Savadkoohi, and C.-H. Lamarque. Study of an electromechanical nonlinear vibration absorber: Design via analytical approach. *Journal of Intelligent Material Systems and Structures*, 32(4):410–419, 2021.

[12] H. Frahm. *Device for damping vibrations of bodies*. US Patent 989,958, 1911.

[13] R. E. Roberson. Synthesis of a nonlinear dynamic vibration absorber. *Journal of the Franklin Institute*, 254(3):205–220, 1952.

[14] A.F. Vakakis, O.V. Gendelman, L.A. Bergman, D.M. McFarland, G. Kerschen, and Y.S. Lee. *Nonlinear targeted energy transfer in mechanical and structural systems*. Springer, Dordrecht, 2008.

[15] O.V. Gendelman, Y. Starosvetsky, and M. Feldman. Attractors of harmonically forced linear oscillator with attached nonlinear energy sink I: description of response regimes. *Nonlinear Dynamics*, 51(1):31–46, 2008.

[16] O. Gendelman, L.I. Manevitch, A.F. Vakakis, and R. M'closkey. Energy pumping in nonlinear mechanical oscillators: part I—dynamics of the underlying hamiltonian systems. *Journal of Applied Mechanics*, 68(1):34–41, 2001.

[17] A.F. Vakakis and O. Gendelman. Energy pumping in nonlinear mechanical oscillators: part II—resonance capture. *Journal of Applied Mechanics*, 68(1):42–48, 2001.

[18] F. Nucera, A.F. Vakakis, D.M. McFarland, L.A. Bergman, and G. Kerschen. Targeted energy transfers in vibro-impact oscillators for seismic mitigation. *Nonlinear Dynamics*, 50(3):651–677, 2007.

[19] O. Gendelman. Analytic treatment of a system with a vibro-impact nonlinear energy sink. *Journal of Sound and Vibration*, 331:4599–4608, 2012.

[20] E. Gourc, G. Michon, S. Seguy, and A. Berlioz. Targeted energy transfer under harmonic forcing with a vibro-impact nonlinear energy sink: Analytical and experimental developments. *Journal of Vibration and Acoustics*, 137(3), 2015.

[21] C.-H. Lamarque, O.V. Gendelman, A. Ture Savadkoohi, and E. Etcheverria. Structural control by means of non-smooth nonlinear energy sink. In *7th European Nonlinear Dynamics Conference (ENOC 2011)*, 2011.

[22] M. Weiss, B. Vaurigaud, A. Ture Savadkoohi, and C.-H. Lamarque. Control of vertical oscillations of a cable by a piecewise linear absorber. *Journal of Sound and Vibration*, 435:281–300, 2018.

[23] G. Hurel, A. Ture Savadkoohi, and C.-H. Lamarque. Design of a nonlinear absorber for a 2 degrees of freedom pendulum and experimental validation. *Structural Control and Health Monitoring*, 28(11):e2814, 2021.

[24] A. Ture Savadkoohi, C.-H. Lamarque, and M.V. Contessa. Trapping vibratory energy of main linear structures by coupling light systems with geometrical and material non-linearities. *International Journal of Non-Linear Mechanics*, 80:3–13, 2016.

[25] C.-H. Lamarque, A. Ture Savadkoohi, and Z. Dimitrijevic. Dynamics of a linear system with time-dependent mass and a coupled light mass with non-smooth potential. *Meccanica*, 49(1):135–145, 2014.

[26] C.-H. Lamarque and A. Ture Savadkoohi. Dynamical behavior of a Bouc-Wen type oscillator coupled to a nonlinear energy sink. *Meccanica*, 49(8):1917–1928, 2014.

[27] B. Cochelin, P. Herzog, and P.-O. Mattei. Experimental evidence of energy pumping in acoustics. *Comptes Rendus Mécanique*, 334(11):639–644, 2006.

[28] R. Bellet, B. Cochelin, P. Herzog, and P.-O. Mattei. Experimental study of targeted energy transfer from an acoustic system to a nonlinear membrane absorber. *Journal of Sound and Vibration*, 329(14):2768–2791, 2010.

[29] V. Alamo Vargas, E. Gourdon, and A. Ture Savadkoohi. Nonlinear softening and hardening behavior in helmholtz resonators for nonlinear regimes. *Nonlinear Dynamics*, 91(1):217–231, 2018.

[30] E. Gourdon, A. Ture Savadkoohi, and V. Alamo Vargas. Targeted energy transfer from one acoustical mode to an helmholtz resonator with nonlinear behavior. *Journal of Vibration and Acoustics*, 140(6):061005 (8), 2018.

[31] M. Volpe, S. Bellizzi, and R. Côte. Polyharmonic distortion approach for nonlinear acoustic load characterization. *Journal of Sound and Vibration*, page 116426, 2021.

[32] X. Guo, H. Lissek, and R. Fleury. Improving sound absorption through nonlinear active electroacoustic resonators. *Phys. Rev. Applied*, 13:014018, 2020.

[33] A.H. Nayfeh and D.T. Mook. *Nonlinear oscillations*. Wiley classics library, 1995.

[34] S. Charlemagne, A. Ture Savadkoohi, and C.-H. Lamarque. Interactions between two coupled nonlinear forced systems: fast/slow dynamics. *International Journal of Bifurcation and Chaos*, 26(09):1650155, 2016.

[35] L.I. Manevitch. The description of localized normal modes in a chain of nonlinear coupled oscillators using complex variables. *Nonlinear Dynamics*, 25:95–109, 2001.

[36] V.V. Smirnov and L.I. Manevitch. Complex envelope variable approximation in nonlinear dynamics. *Russian Journal of Nonlinear Dynamics*, 16(3):491–515, 2020.

[37] L.I. Manevitch and O.V. Gendelman. *Tractable Models of Solid Mechanics*. Foundations of Engineering Mechanics. Springer-Verlag Berlin Heidelberg, 2011.

[38] A. Ture Savadkoohi, C.-H. Lamarque, M. Weiss, B. Vaurigaud, and S. Charlemagne. Analysis of the 1:1 resonant energy exchanges between coupled oscillators with rheologies. *Nonlinear Dynamics*, 86(4):2145–2159, 2016.

[39] A. Luongo, D. Zulli, and G. Piccardo. Analytical and numerical approaches to nonlinear galloping of internally resonant suspended cables. *Journal of Sound and Vibration*, 315(3):375–393, 2008.

[40] J. Awrejcewicz, R. Starosta, and G. Sypniewska-Kamińska. Asymptotic analysis of resonances in nonlinear vibrations of the 3-dof pendulum. *Differential Equations and Dynamical Systems*, 21(1):123–140, 2013.

[41] R. Starosta, G. Sypniewska-Kamińska, and J. Awrejcewicz. Quantifying non-linear dynamics of mass-springs in series oscillators via asymptotic approach. *Mechanical Systems and Signal Processing*, 89:149–158, 2017.

[42] C. Bertrand, A. Ture Savadkoohi, and C.-H. Lamarque. Nonlinear oscillations of a pendulum cable with the effects of the friction and the radius of the support. *Nonlinear Dynamics*, 96(2):1303–1315, 2019.

[43] J. Awrejcewicz, R. Starosta, and G. Sypniewska-Kamińska. Complexity of resonances exhibited by a nonlinear micromechanical gyroscope: an analytical study. *Nonlinear Dynamics*, 97(3):1819–1836, 2019.

[44] V. Guillot, A. Ture Savadkoohi, and C.-H. Lamarque. Analysis of a reduced-order nonlinear model of a multi-physics beam. *Nonlinear Dynamics*, 97(2):1371–1401, 2019.

[45] J. Awrejcewicz, R. Starosta, and G. Sypniewska-Kamińska. Nonlinear vibration of a lumped system with springs-in-series. *Meccanica*, 56(4):753–767, 2021.

[46] A. Casalotti, D. Zulli, and A. Luongo. Dynamic response to transverse loading of a single-layered tubular beam via a perturbation approach. *International Journal of Non-Linear Mechanics*, 137:103822, 2021.

[47] E. Gourdon, N.A. Alexander, C.A. Taylor, C.-H. Lamarque, and S. Pernot. Nonlinear energy pumping under transient forcing with strongly nonlinear coupling: Theoretical and experimental results. *Journal of Sound and Vibration*, 300(3):522–551, 2007.

[48] A. Ture Savadkoohi, B. Vaurigaud, C.-H. Lamarque, and S. Pernot. Targeted energy transfer with parallel nonlinear energy sinks, part II: theory and experiments. *Nonlinear Dynamics*, 67(1):37–46, 2012.

[49] N.E. Wierschem, S.A. Hubbard, J. Luo, L.A. Fahnestock, B.F. Spencer, D.M. McFarland, D.D. Quinn, A.F. Vakakis, and L.A. Bergman. Response attenuation in a large-scale structure subjected to blast excitation utilizing a system of essentially nonlinear vibration absorbers. *Journal of Sound and Vibration*, 389:52–72, 2017.

[50] Y. S. Lee, A. F. Vakakis, L. A. Bergman, D. M. McFarland, and G. Kerschen. Suppression aeroelastic instability using broadband passive targeted energy transfers, part I: Theory. *AIAA journal*, 45(3):693–711, 2007.

[51] Y. S. Lee, G. Kerschen, D. M. McFarland, W. J. Hill, C. Nichkawde, T. W. Strganac, L. A Bergman, and A. F. Vakakis. Suppressing aeroelastic instability using broadband passive targeted energy transfers, part II: experiments. *AIAA journal*, 45(10):2391–2400, 2007.

Detection of different dynamics of two coupled oscillators including
a time-dependent cubic nonlinearity
A PREPRINT

[52] O.V. Gendelman, A.F. Vakakis, L.A. Bergman, and D.M. McFarland. Asymptotic analysis of passive nonlinear suppression of aeroelastic instabilities of a rigid wing in subsonic flow. *SIAM Journal on Applied Mathematics*, 70(5):1655–1677, 2010.

[53] B. Vaurigaud, L.I. Manevitch, and C.-H. Lamarque. Passive control of aeroelastic instability in a long span bridge model prone to coupled flutter using targeted energy transfer. *Journal of Sound and Vibration*, 330(11):2580–2595, 2011.

[54] A. Luongo and D. Zulli. Aeroelastic instability analysis of NES-controlled systems via a mixed multiple scale/harmonic balance method. *Journal of Vibration and Control*, 20(13):1985–1998, 2014.

[55] C.-H. Lamarque, O.V. Gendelman, A. Ture Savadkoohi, and E. Etcheverria. Targeted energy transfer in mechanical systems by means of non-smooth nonlinear energy sink. *Acta mechanica*, 221(1):175–200, 2011.

[56] Y. Starosvetsky and O.V. Gendelman. Strongly modulated response in forced 2dof oscillatory system with essential mass and potential asymmetry. *Physica D: Nonlinear Phenomena*, 237(13):1719–1733, 2008.